

RATIONAL DESIGN OF BITUMINOUS PAVING MIXTURES WITH CURVED MOHR ENVELOPES

NORMAN W. McLEOD

INTRODUCTION

In a paper presented at the annual meeting of this Association about two years ago, the writer outlined a rational approach to the design of bituminous paving mixtures based on the triaxial test. This method was limited to bituminous paving mixtures for which the triaxial data provide straight line Mohr envelopes.

While triaxial data for a great many bituminous paving mixtures can be best represented by straight line Mohr envelopes, it appears that there are certain bituminous mixtures for which a curved Mohr envelope is obtained when the triaxial data are plotted. It is with this latter case that the present paper is chiefly concerned.

A rational approach to the design of bituminous pavements can be defined as a method for determining or expressing their strength or stability in terms of pounds per square inch or some other unit stress basis, similar to those employed for indicating the strength of steel, concrete, etc. The study leading to this rational approach was undertaken to investigate the design requirements for bituminous pavements in general, but especially for those capable of supporting tire pressures of 300, 400, 500 psi • 9 etc ., under consideration for future aircraft, and in particular to attempt to determine the minimum c and ϕ values required by bituminous mixtures to support various wheel loads and tire pressures.

In view of the common current use of empirical tests such as Marshall, Hveem Stabilometer, and Hubbard-Field, it might be asked why there should be any interest in endeavouring to develop a rational method of design for bituminous pavements. This query can be answered by another question. What Hveem Stabilometer rating* should be specified for a bituminous pavement intended to carry a tire pressure of 400 psi., for example, or what **Hubbard-Field** or **Marshall** stability value? No suitable answer to this question can be given until the stability values for bituminous mixtures measured by each of these empirical tests have been correlated with test sections that have performed adequately when

*Engineering Consultant, Department of Transport, Ottawa, Canada.

subjected to traffic by tires inflated to 400 psi. On the other hand, if we had a satisfactory rational method of design for bituminous pavements, it would be no more difficult to design bituminous paving mixtures of adequate stability for tire pressures of 100, 200, 400 psi., etc., than it now is to design bridges of the required strength regardless of whether the span is to be 50 feet, 500 feet, or 5,000 feet, etc.

In addition, we do not know what safety factors these empirical methods are actually employing. Furthermore, they may be rejecting paving mixtures that would actually develop the stability required and may be permitting and even encouraging the use of others that will not always be stable in the field.

Finally, a rational method of design, because of its theoretical background, is able to suggest possible solutions to certain design problems in any engineering field that would not even be dreamed about on the basis of empirical tests. That the design of bituminous pavements is no exception to this will be demonstrated later in the present paper.

BITUMINOUS MIXTURES WITH STRAIGHT MOHR ENVELOPES

Before outlining a rational approach to the design of bituminous paving mixtures with curved Mohr envelopes, it is necessary to review some of the important subject matter from three earlier papers (1,2,3) which described a rational approach to the design of bituminous paving mixtures with straight line Mohr envelopes.

It was assumed in these earlier papers (1,2,3), as it will be in this, that the thickness of base course and surface is adequate to prevent **subgrade** failure and that the base course material itself will not fail under the shearing stresses imposed by any of the applied loads, Figure 1. The problem under consideration, therefore, is the development of a rational method for designing bituminous paving mixtures that will have sufficient strength or stability to resist failure (being squeezed out between tire and base course) under the wheel loads and tire pressures to which they are to be subjected. These paving mixtures are assumed to have been properly designed in every other respect, such as workability, density, durability, etc.

Very often the first important step toward the solution of a problem has been taken if the nature of the problem has been clearly outlined. It is possible that the development and continued use of empirical tests such as Marshall, Hveem, and **Hubbard-**

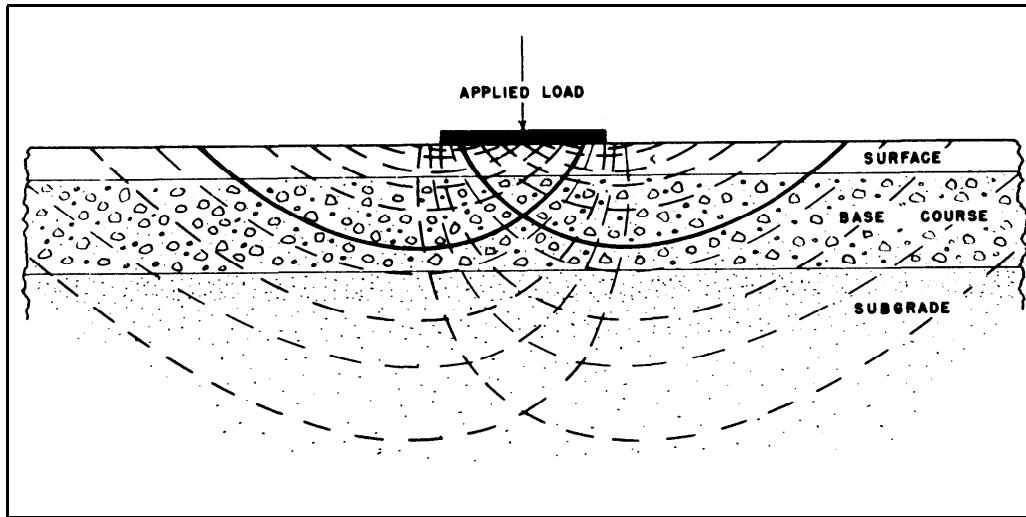


Fig. 1. Diagram of Shear Planes Under a Loaded Area.

Field, is due at least in part to the failure of bituminous paving engineers to clearly recognize the precise nature of the bituminous pavement stability problem. In Figure 2(a), the change in pressure across the transverse axis of the contact area of a tire resting on a pavement is indicated by the line labelled tire pressure curve. The pressure rises rapidly from zero at either edge of the contact area to a peak maximum thought to be due to the walls of the tire, and then drops slightly from these peaks toward the centre. This shape for the tire pressure curve is indicated by the work of Teller and Buchanan (4) and of O. J. Porter (5), although Markwick and Starks (6) believe as a result of their measurements that the two peaks shown in Figure 2(a) do not occur, and that the pressure continues to increase slightly toward the centre for both stationary and moving tires, instead of decreasing as illustrated in Figure 2(a). It is apparent, therefore, that more experimental work is required to investigate the shape of the curve of tire pressure across the contact area.

Assuming that the tire pressure curve shown in Figure 2(a) is reasonably representative, the nature of the stability problem becomes quite apparent. Most engineers would probably require that the stability developed by the bituminous pavement at all points on the contact area must be at least equal to the pressure applied by the tire at each of these points, Figure 2(b). That is, the stability curve must not cut through the pressure curve at any point, since the pavement would tend to be unstable for the portion of the contact area for which the stability curve was below the pressure curve. The critical stability curve, therefore, is the one that is just tangent to the pressure curve illustrated in

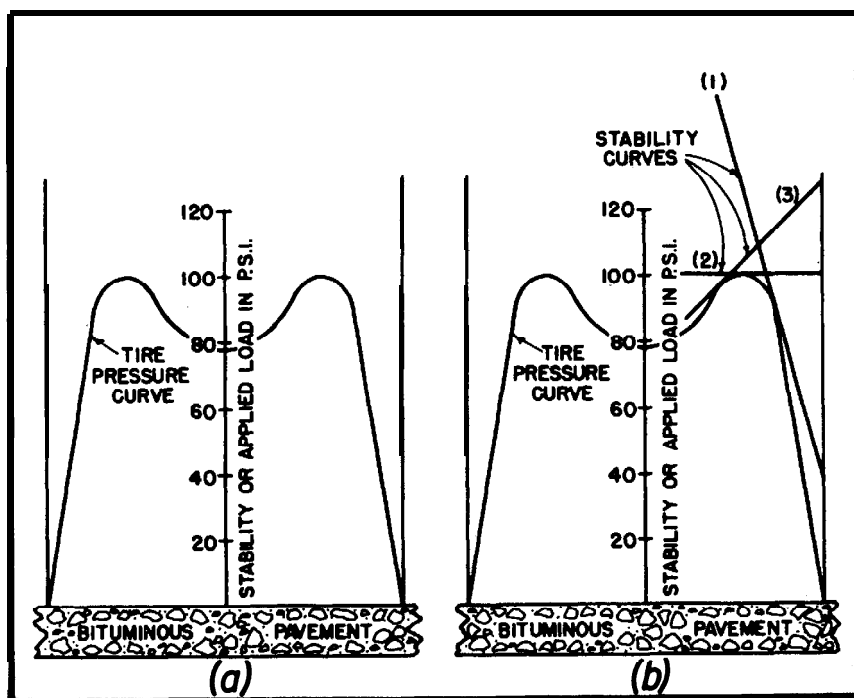


Fig. 2. Diagram Illustrating the Nature of the Stability Problem for Bituminous Paving Mixtures.

Figure 2(b). The question arises as to which of the three straight lines of positive, zero, and negative slope drawn tangent to the tire pressure curve in Figure 2(b) is the critical stability curve. It was demonstrated earlier (1,2,3) that the critical stability curve tends to be a curved rather than a straight line, and that it generally slopes upward from a point at the edge of the contact area. The stability problem, therefore, requires the development of a method for determining the shape, location, and slope of the stability curve for any bituminous pavement, and comparing it with the severest loading in the form of a tire pressure curve to which the pavement is likely to be subjected, Figure 2(b). It should be noted in passing that it is not possible to plot the stability value given by any one of three empirical tests, **Hubbard-Field**, **Hveem Stabilometer**, or **Marshall**, for a bituminous paving mixture, as a stability curve, or even as a single point on the diagram of Figure 2(b). That is, the stability value given by any one of these tests for a bituminous paving mixture cannot be compared directly with the curve of the tire pressure to be applied to the pavement.

It was pointed out in the earlier papers (1,2,3), that the stability requirements for a bituminous paving mixture depend upon whether the applied wheel load is: (a) static or moving very

slowly, e.g., parking areas, taxiways, etc.; (b) moving rapidly at uniform speed, e.g., rural highways or the central portion of airport runways; or (c) subjecting the pavement to severe braking or acceleration stresses, e.g., stop lights, bus stops.

The assumption was made that the strength characteristics of a bituminous paving mixture are indicated by the magnitudes of the values of cohesion c and angle of internal friction ϕ , given by the Mohr diagram based upon triaxial test data for the mixture, Figure 3. It was pointed out that an increase in the rate of strain employed in the triaxial test results in an increase in the value of cohesion c , due to the viscous resistance of the paving mixture, but has little or no effect on the value of the angle of internal friction ϕ . This provides a rational explanation for the greater stability shown by bituminous paving mixtures under rapidly moving as compared with static or slowly moving wheel loads, that has been demonstrated by field experience.

It should be mentioned that an important objective of a rational method of design for bituminous paving mixtures on the basis of the triaxial test is to determine the smallest corresponding values of c and ϕ needed to provide a stable bituminous pavement for the most critical loading conditions (wheel load and tire pressure) anticipated throughout its lifetime. The smaller the corresponding values required for c and ϕ , the wider is the range of

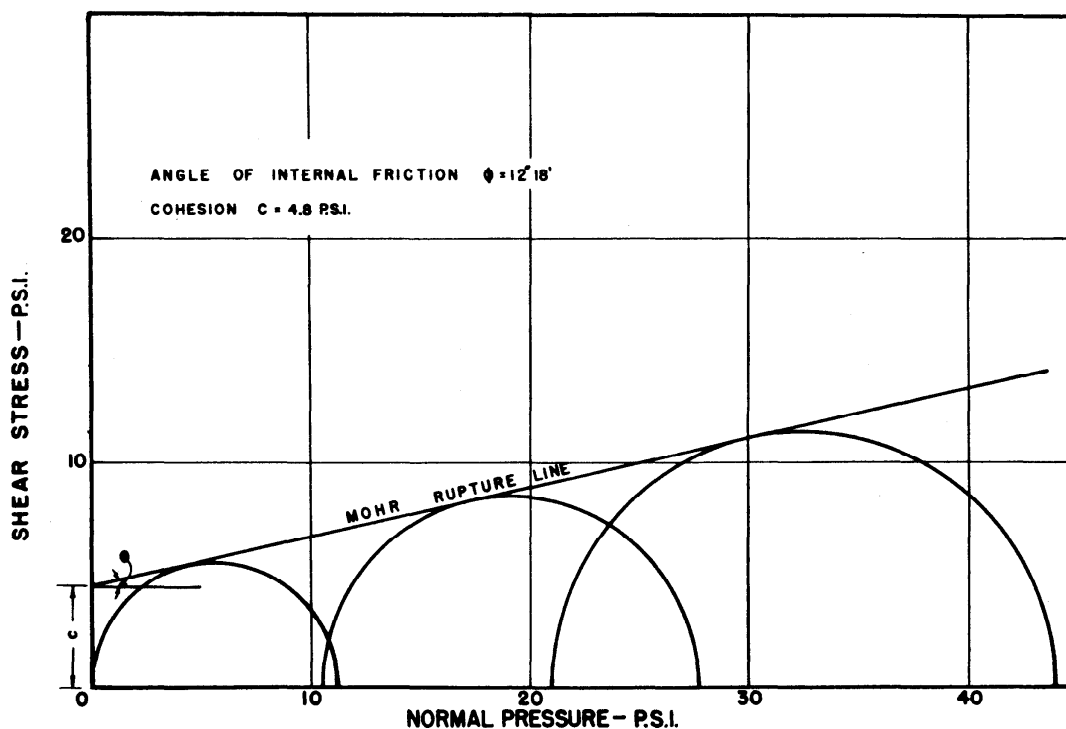


Fig. 3. Typical Mohr Diagram for Triaxial Compression Test.

aggregates from which a selection may be made to provide a bituminous pavement of adequate stability. This in turn tends to lower the cost of bituminous pavement construction.

It was assumed that the stresses involved when a loaded tire rests on a bituminous pavement are equivalent to those of a strip load of great length. Since it was shown that the pavement under a loaded tire develops more stability in the direction of the longitudinal than the transverse axis of the contact area, this assumption is not unreasonable. However, because the actual length of the tire contact area on a pavement is relatively short, this assumption leads to somewhat conservative design.

It was pointed out that, all other factors being equal, the stability of a bituminous pavement appears to depend very materially upon:

- (1) the lateral support of the pavement adjacent to the loaded area, L_S ;
- (2) the frictional resistance between pavement and tire and between pavement and base, which can be expressed as an equivalent lateral support L_R ;
- (3) the shape of the curve of tire pressure distribution over the contact area.

On the basis of the geometry of the Mohr diagram (Figure 3), the maximum vertical load V that a bituminous pavement can support is given by the following equation:

$$v = 2c \sqrt{\frac{1 + \sin \phi}{1 - \sin \phi}} + L \left(\frac{1 + \sin \phi}{1 - \sin \phi} \right) \quad (1)$$

where c = cohesion c obtained directly from the Mohr diagram,
 ϕ = angle of internal friction ϕ obtained directly from the Mohr diagram, and

L = the total effective lateral support from all sources that can be mobilized to react against the lateral thrust of the prism of pavement immediately under the loaded area.

The significance of equation (1) is illustrated by Figure 4. The right hand side of equation (1) demonstrates that the stability V of a material with both cohesion c and angle of internal friction ϕ consists of two items. The first of these, $2c \sqrt{\frac{1 + \sin \phi}{1 - \sin \phi}}$, represents the unconfined compressive strength of the material and is illustrated by either of Mohr circles OV' or $V''V$ in Figure 4(b). The second term, $L \left(\frac{1 + \sin \phi}{1 - \sin \phi} \right)$, defines the stability of a purely

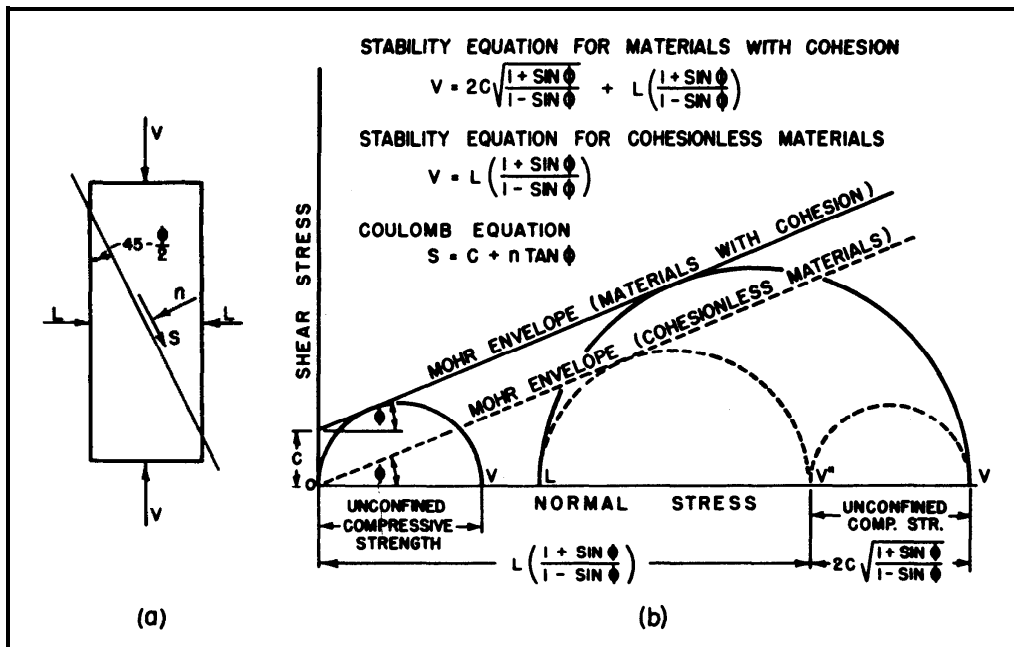


Fig. 4. Illustrating the Physical Significance of the Equation 01 Stability Provided by the Mohr Diagram.

cohesionless material; that is, a material for which the Mohr envelope goes through the origin. Consequently, for any given lateral pressure L , the stability V of a cohesive material is made up of V'' , the stability of a corresponding cohesionless material having the same angle of internal friction ϕ , plus the unconfined compressive strength of the cohesive material, represented by either OV' or $V''V$. Expressed in another way, the difference in stability between a purely cohesionless material with a given angle of internal friction ϕ , and a material having both cohesion c and the same angle of internal friction ϕ , is the unconfined compressive strength of the latter material.

That the lateral pressure L should influence only the frictional element of resistance represented by the angle of internal friction ϕ , even in a material with both c and ϕ , is clear from an examination of Figure 4(a) and the Coulomb equation. When the lateral pressure $L = 0$, the maximum vertical load V that the element of Figure 4(a) can sustain is equal to its unconfined compressive strength. When the lateral support L has some positive value, the normal stress n on the plane of failure of the element is increased, Figure 4(a), and the maximum vertical load V that can be supported without failure is also correspondingly increased. However, the Coulomb equation, $s = c + n \tan \phi$, indicates that this increase in normal pressure n on the plane of failure influences only the frictional element of the shearing resistance of the

material represented by $\tan \phi$. Consequently, although it has no effect on the cohesive element of resistance of a material, the lateral support L contributes to a greater vertical failure load or stability V , because it has a direct influence on the frictional element of resistance.

One source of lateral support L is quite obviously provided by the pavement immediately adjacent to and surrounding the contact area. This portion of the total effective lateral support L is designated by L_S . As previously explained (1,2,3), and as illustrated by Figure 5, the unconfined compressive strength of the bituminous paving mixture can probably be taken as a conservative measure of the lateral support L_S provided by the pavement immediately adjacent to the loaded area; that is (from the Mohr diagram),

$$L_S = 2c \sqrt{\frac{1 + \sin \phi}{1 - \sin \phi}} \quad (2)$$

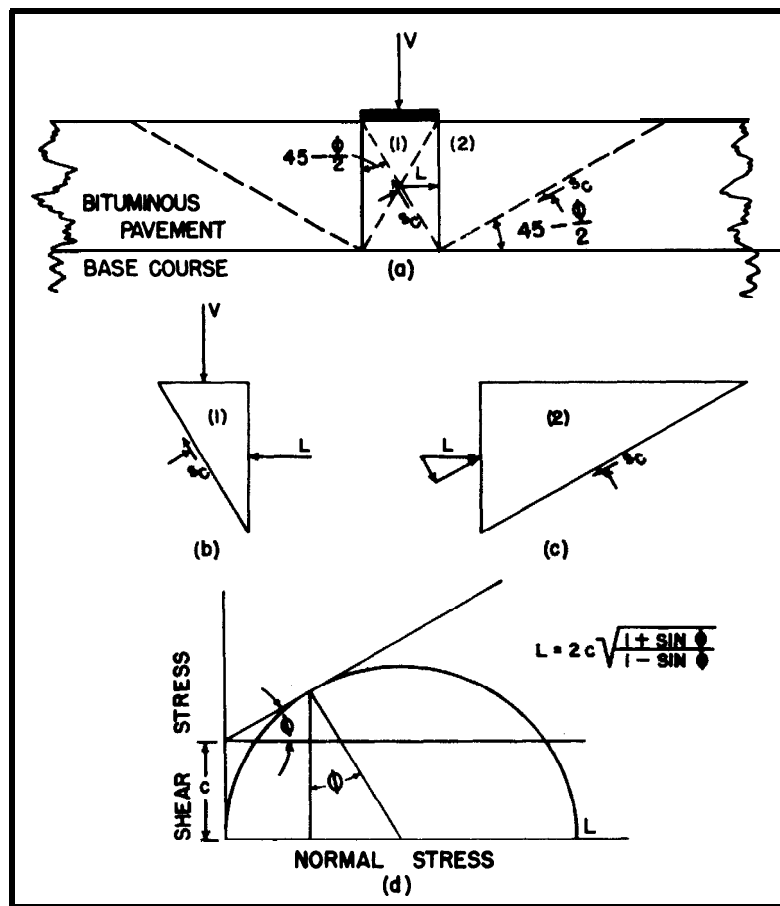


Fig. 5. Illustrating that the Lateral Support L Provided by the Portion of a Bituminous Pavement Surrounding the Loaded Area

Is Given by $L = 2c \sqrt{\frac{1 + \sin \phi}{1 - \sin \phi}}$.

If this value for L_S is substituted for L in equation (1), the following equation results after substitution and simplification,

$$V = \frac{4c}{1 - \sin \phi} \sqrt{\frac{1 + \sin \phi}{1 - \sin \phi}} \tag{3}$$

The Mohr diagram illustrating the values of V in equation (3) is shown in Figure 6, wherein the Mohr circle on the left represents the unconfined compressive strength.

Figure 7 provides a graphical representation of equation (3) for a wide range of tire pressures. It should be emphasized that Figure 7 illustrates a diagram for the design of bituminous paving mixtures on the basis that the only source of lateral support L is that provided by the portion of the pavement adjacent to the loaded area, and that L is equal to the unconfined compressive strength of the paving mixture in each case.

It was indicated previously (1,2,3) that due to several other sources of resistance, the actual value of the lateral support L_S provided by the pavement surrounding the loaded area is probably greater than the unconfined compressive strength of the paving mixture. It was suggested that these additional sources of resistance outside of the loaded area could be taken into account by making L_S equal to the unconfined compressive strength multiplied by a factor K , when it would become

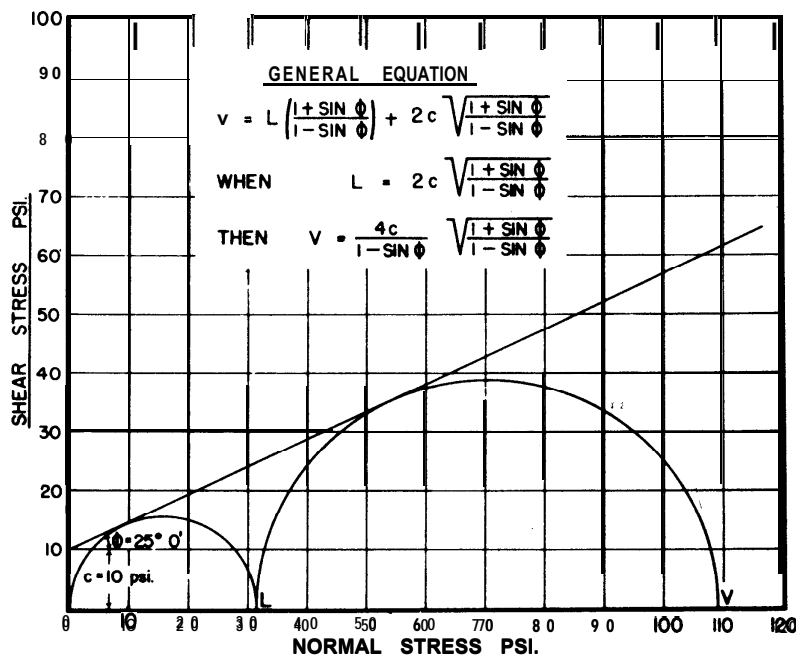


Fig. 6. Diagram Illustrating Maximum Vertical Load V that Can Be Carried by a Bituminous Pavement when Lateral Support L Is Equal to the Unconfined Compressive Strength of the Material.

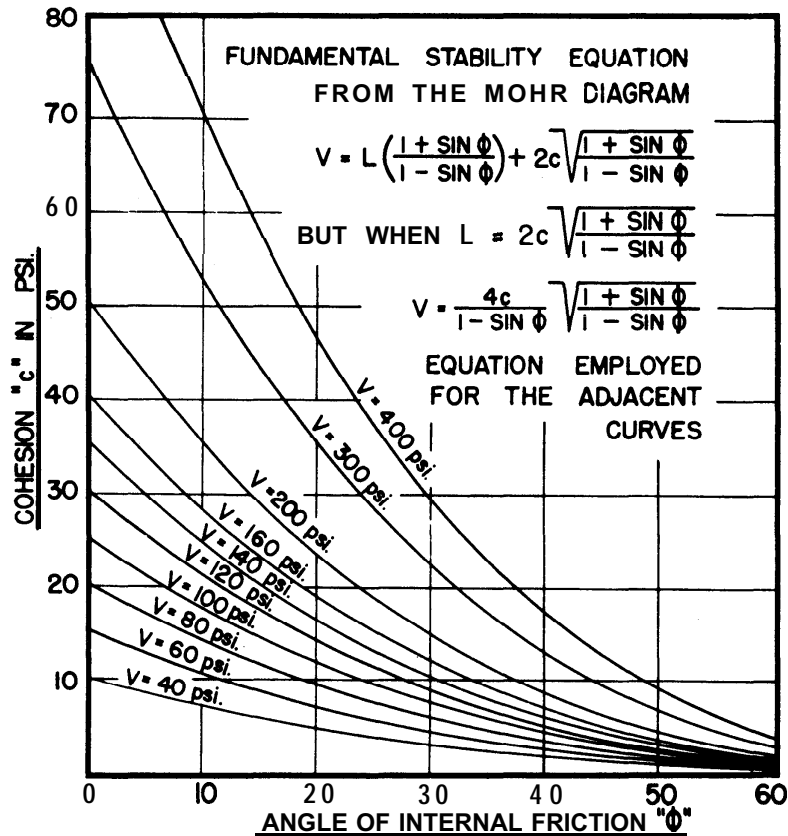


Fig. 7. Design Chart for Bituminous Mixtures Based on Tri-axial Test and Values of Lateral Support $L = 2c \sqrt{\frac{1 + \sin \phi}{1 - \sin \phi}}$.

$$L_S = 2cK \sqrt{\frac{1 + \sin \phi}{1 - \sin \phi}} \quad (4)$$

Substituting the right hand side of equation (4) for L in equation (1) and simplifying, gives the following:

$$V = 2c \sqrt{\frac{1 + \sin \phi}{1 - \sin \phi}} \left(\frac{K (1 + \sin \phi) + (1 - \sin \phi)}{1 - \sin \phi} \right) \quad (5)$$

which reduces to equation (3) when K is taken equal to unity. When V refers to the ultimate strength of the pavement, K = 1 would probably be a conservative value for K, and it is assumed to have this value in the equations and diagrams employed to illustrate the principles under discussion in the present paper. Later on, when sufficient data become available, K can be evaluated more definitely for actual design, and the appropriate value for K might turn out to be either less or greater than unity.

The three previous papers pointed out that the frictional resistance between pavement and tire, and between pavement and

base, seem to provide an additional major source of pavement stability. Figure 8 illustrates the nature and location of these two frictional resistances, and Figures 8(b) and 9 indicate that they can be represented mathematically by an equivalent additional lateral support L_R .

Values of the coefficient of friction f between pavement and tire have been measured by Moyer (7) and Lee (8), who report values of f up to 1.0 for stationary or slowly moving vehicles, although 0.8 is a more normal top value. No data seem to be presently available concerning the value of g , the coefficient of friction between pavement and base. For a rational method of design, values for f and g must be either determined or assumed for pavement design for each individual project.

Figure 9 illustrates a method for evaluating the total frictional resistance between pavement and tire and between pavement and base in terms of the equivalent lateral support L , and for expressing the maximum value of L_R that can be developed as a simple mathematical equation,

$$L_R = n(P + Q)(c + V \tan \phi) \left(\tan \left(45 - \frac{\phi}{2} \right) \right) \quad (6)$$

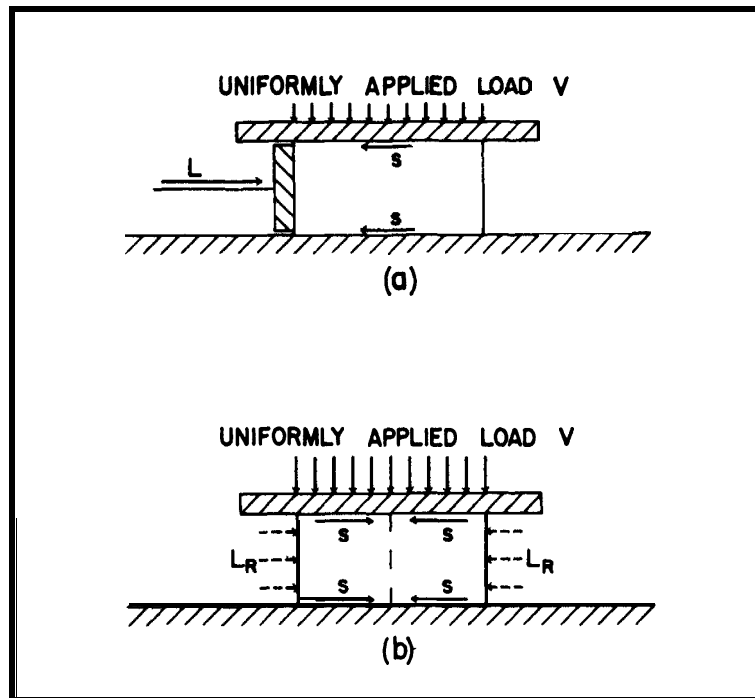


Fig. 8. Diagram Illustrating that Friction Between Tire and Pavement and Between Pavement and Base Is Equivalent to Additional Lateral Support for the Section of Pavement Under a Loaded Area.

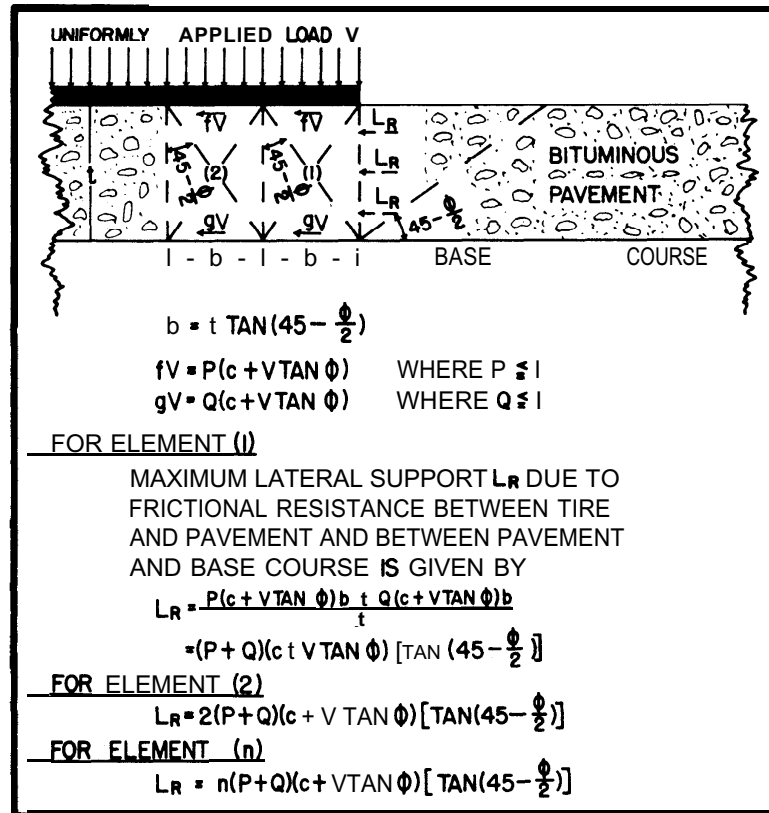


Fig. 9. Diagram Illustrating the Magnitude of the Lateral Support L_R Equivalent to the Frictional Resistance Developed Between Tire and Pavement and Between Pavement and Base, Under the Loaded Area.

Figure 9 explains that the factor P in equation (6) indicates that the maximum frictional resistance fV that can be developed between pavement and tire cannot exceed the shearing resistance of the bituminous pavement itself, which is given by the Coulomb equation $s = c + V \tan \phi$, where V is the pressure applied by the tire to the contact area. The factor Q is of similar significance with respect to the frictional resistance gV between pavement and base. As shown by Figure 9, the highest value that either P or Q can have individually is unity, and the lowest value is zero. Therefore, the maximum value for $P + Q = 2$, and the minimum value is zero.

In actual practice it may be found that either P or Q can develop a larger value than unity. However, since there is no present reason for expecting this, it is assumed that neither P nor Q can have values greater than unity.

Equation (6) can be rewritten in terms of f and g , rather than P and Q , when it becomes,

$$L_R = nV (f + g) \left(\tan \left(45 - \frac{\phi}{2} \right) \right) \quad (7)$$

It is apparent that the total effective lateral support L developed by a bituminous pavement can be expressed as

$$L = L_S + L_R \quad (8)$$

from which it follows that equation (1) can be rewritten as

$$V = 2c \sqrt{\frac{1 + \sin \phi}{1 - \sin \phi}} + L_S \left(\frac{1 + \sin \phi}{1 - \sin \phi} \right) + L_R \left(\frac{1 + \sin \phi}{1 - \sin \phi} \right) \quad (9)$$

Equation (9) makes it clear that the stability of a bituminous pavement consists of three principal parts :

- (a) The stability due to unconfined compressive strength of the pavement represented by the first term on the right hand side, $2c \sqrt{\frac{1 + \sin \phi}{1 - \sin \phi}}$. This might be referred to as the inherent strength of the pavement in the complete absence of lateral support from the surrounding material, and of frictional resistance between pavement and tire and between pavement and base.
- (b) Stability due to the lateral support L_S provided by the portion of the pavement adjacent to the loaded area, and expressed by the term $L_S \left(\frac{1 + \sin \phi}{1 - \sin \phi} \right)$.
- (c) Stability due to a lateral support L_R equivalent to the frictional resistance between pavement and tire and between pavement and base, and represented by the term $L_R \left(\frac{1 + \sin \phi}{1 - \sin \phi} \right)$.

In addition, a further source of stability in the form of arching action, particle interference, etc., due to their composition and thickness, may exist in certain bituminous pavements. This could be referred to as structural stability. Where it exists, structural stability might be evaluated as the difference between the total stability developed, and the stability calculated on the basis of equations (10) and (11).

Since L_S has already been evaluated by equation (4), and L_R by equation (6), and remembering that the pressure exerted by a tire is not uniform, but varies across the contact area (4,5), e.g., Figure 2, equation (9) can be written as follows:

$$V = 2c \sqrt{\frac{1 + \sin \phi}{1 - \sin \phi}} + 2cK \sqrt{\frac{1 + \sin \phi}{1 - \sin \phi}} \left(\frac{1 + \sin \phi}{1 - \sin \phi} \right) + n(P + Q)(c + V' \tan \phi) \left(\tan \left(45 - \frac{\phi}{2} \right) \right) \left(\frac{1 + \sin \phi}{1 - \sin \phi} \right) \quad (10)$$

where V = stability in psi. developed by the bituminous pavement at any point on the contact area,

c = unit cohesion in psi. obtained from the Mohr diagram,

ϕ = angle of internal friction obtained from the Mohr diagram,

K = a constant, which may be taken equal to unity for conservative design,

P = ratio of frictional resistance fV between pavement and tire to the shearing resistance of the pavement represented by the Coulomb equation $s = c + V \tan \phi$, and, therefore, has a maximum value of unity,

Q = ratio of frictional resistance gV between pavement and base to the shearing resistance of the pavement $c + V \tan \phi$, and has a maximum value of unity,

n = the number of elements, each of width equal to $t \left(\tan \left(45 - \frac{\phi}{2} \right) \right)$, measured from the edge of the contact area to the point on the contact area where the value of stability V is required, where t is the thickness of pavement,

V' = the average vertical pressure exerted by the tire between the edge and the point on the contact area at which the value of stability V is required.

When L_R is represented by equation (7) instead of equation (6), equation (10) becomes,

$$V = 2c \sqrt{\frac{1 + \sin \phi}{1 - \sin \phi}} + 2cK \sqrt{\frac{1 + \sin \phi}{1 - \sin \phi}} \left(\frac{1 + \sin \phi}{1 - \sin \phi} \right) + nV'(f + g) \left(\tan \left(45 - \frac{\phi}{2} \right) \right) \left(\frac{1 + \sin \phi}{1 - \sin \phi} \right) \quad (11)$$

where f = coefficient of friction between pavement and tire,

g = coefficient of friction between pavement and base, and the other symbols have the significance previously defined for them.

In Figure 9 and equations (6), (7), (10), and (11), the quantity " n " occurs. It measures the distance " d " from the edge to any point " x " on the contact area as the number of unit elements each

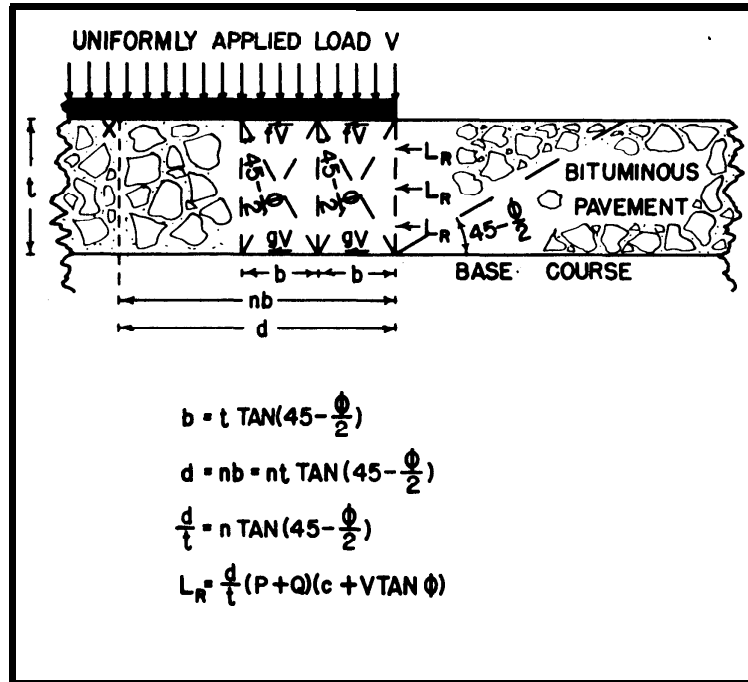


Fig. 10. Illustrating Magnitude of Lateral Support L_R When $\frac{d}{t}$ Is Substituted for $n \tan \left(45 - \frac{\phi}{2} \right)$.

of width, "b", where $b = t \tan \left(45 - \frac{\phi}{2} \right)$; that is, from Figure 10,

$$d = nb = nt \tan \left(45 - \frac{\phi}{2} \right) \tag{12}$$

or
$$\frac{d}{t} = n \tan \left(45 - \frac{\phi}{2} \right) \tag{13}$$

Consequently, $\frac{d}{t}$ may be substituted for $n \tan \left(45 - \frac{\phi}{2} \right)$ in equations (6), (7), (10), and (11). When this substitution is made, equation (6) becomes

$$L_R = \left(\frac{d}{t} \right) (P + Q) (c + V \tan \phi) \tag{14}$$

equation (7) becomes

$$L_R = \left(\frac{dV}{t} \right) (f + g) \tag{15}$$

equation (10) becomes

$$\begin{aligned}
 V = & 2c \sqrt{\frac{1 + \sin \phi}{1 - \sin \phi}} + 2cK \sqrt{\frac{1 + \sin \phi}{1 - \sin \phi}} \left(\frac{1 + \sin \phi}{1 - \sin \phi} \right) \\
 & + \frac{d}{t} (P + Q) (c + V' \tan \phi) \left(\frac{1 + \sin \phi}{1 - \sin \phi} \right) \tag{16}
 \end{aligned}$$

and equation (11) becomes

$$v = 2c \sqrt{\frac{1 + \sin \phi}{1 - \sin \phi}} + 2cK \sqrt{\frac{1 + \sin \phi}{1 - \sin \phi}} \left(\frac{1 + \sin \phi}{1 - \sin \phi} \right) + \left(\frac{dV'}{t} \right) (f+g) \left(\frac{1 + \sin \phi}{1 - \sin \phi} \right) \quad (17)$$

The pavement thickness "t" appears directly in equations (14), (15), (16), and (17), but only indirectly in equations (6), (7), (10), and (11), and might be favoured by some for that reason. Both sets of equations are equivalent to each other in every respect, and provide identical solutions to any given problem.

That the frictional resistance fV between pavement and tire and the frictional resistance gV between pavement and base may be an important source of stability for bituminous pavements, is illustrated by Figure 11, in which the straight line stability curves for various values of $P + Q$ and $f + g$ indicate a rapid increase of pavement stability when proceeding from the edge toward the centre of the contact area. For Figure 11 it was assumed that a uniform tire pressure of 100 psi. was applied to the contact area, and that

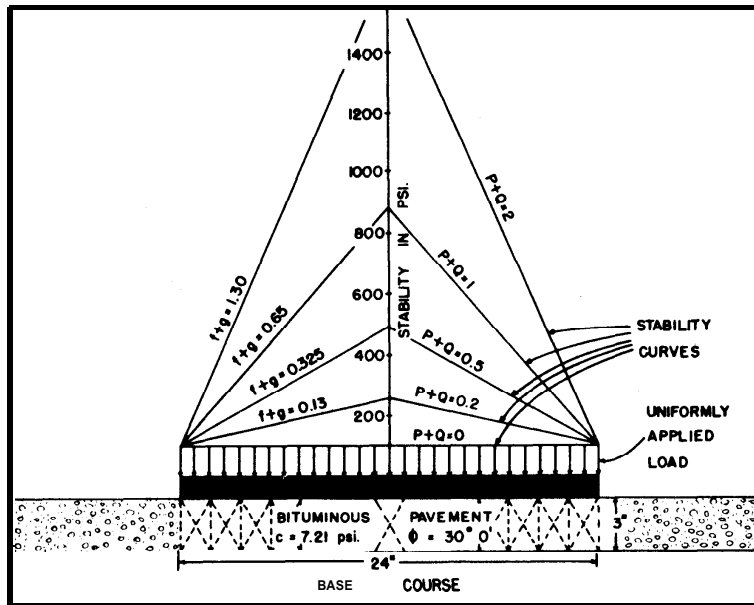


Fig. 11. Relationships Between Applied Load and Stability of Bituminous Pavements at Varying Distances from Edge Under the Loaded Area and for Different Degrees of Frictional Resistance Developed Between Pavement and Tire and Between Pavement and Base. (Pavement Stability Equal to Applied Load for Edge Conditions.) Aeroplane Tire.

the stability of the pavement was exactly 100 psi. at the edge of the contact area, due to the first two terms on the right hand side of equations (9), (10), (11), (16), and (17). The increase in stability of the pavement underlying the loaded area when proceeding from the edge to the centre of the contact area, illustrated by the stability curves in Figure 11, was calculated by means of the third term on the right hand side of equations (10) or (16) for the $P + Q$ curves, and by means of the third term on the right hand side of equations (11) or (17) for the stability curves labelled with $f + g$ values. Figure 11 demonstrates that even a low value for $f + g = 0.325$ raises the stability of the pavement near the centre of the contact area to more than four times its stability at the edge, for the particular conditions pertaining to this diagram.

Other evidence of the considerable influence of frictional resistance between pavement and tire and between pavement and base on the stability of bituminous mixtures is provided by the fact that Jurgenson (9) designed a test for measuring the shearing resistance of clay, by squeezing it between two rough surfaces, e.g., Figure 8. In this case, also, the maximum shear is developed at each of the two interfaces.

As a further check on the importance of these two frictional resistances, the load was applied to a layer of plasticine (a modeling clay) 0.75 inch thick and resting on a large steel plate, by means of steel bearing plates 3, 6, 9, and 12 inches in diameter. Some very preliminary results are shown graphically in Figure 12 for a vertical deformation of 0.05 inch in each case. They indicate that due to the greater distance between centre and edge over which the two frictional resistances are acting as the bearing plate diameter is increased, the load carried by the 12 inch plate, 57.5 psi., is over two and one-half times the load carried by the 3 inch plate, 22.4 psi. It will be recalled that for load tests at the surface of a great depth of clay, the unit pressure supported at any given deflection decreases with increasing diameter of the bearing plate, and that the curve of unit pressure versus plate diameter would slope down from the 3-inch plate, instead of sloping upward as in Figure 12. Consequently, the influence of the frictional resistances between the plasticine and the upper and lower bearing surfaces on the strength or stability developed by the plasticine is even greater than Figure 12 may indicate as a first impression. It should be emphasized again that Figure 12 represents the results of some very preliminary tests, which will be repeated much more carefully at an early date.

Many fine examples of the important influence of good frictional resistance between pavement and base on pavement stability

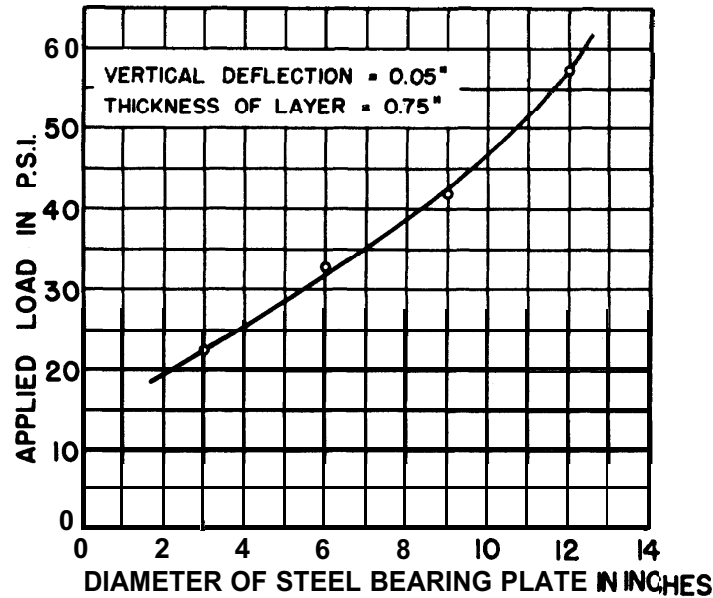


Fig. 12. Increase in Supporting Value of Plasticine Layer with Increase in Diameter of Bearing Plate.

have been provided by field experience. An otherwise well-designed paving mixture, when laid on a smooth base, or on a base to which it is poorly bonded or not at all, will quickly develop indications of instability under traffic, quite often in the form of large tension cracks of well-recognized pattern.

Figure 13 illustrates the application of equations (10) or (16) and (11) or (17) to the actual design of a bituminous paving mixture. The heavy continuous curve represents the actual pressure applied to the pavement by the tire at all points across the transverse axis of the contact area (4,5).

The short curves on the right and left hand sides of Figure 13 are stability curves for different values of $f + g$ for a given paving mixture for which $c = 6.9$ psi. and $\theta = 25^\circ$, as indicated. The positions of these stability curves are located by applying equations (10) or (16) and (11) or (17). The location of the stability curve at the edge of the contact area (75 psi.) is calculated by means of the first two terms on the right hand side of these equations; that is, on the basis that the only source of pavement stability is the unconfined compressive strength of the pavement (the first term on the right hand side of equations (10) or (16) and (11) or (17)), plus the stability due to the lateral support provided by the pavement adjacent to the loaded area (the second term on the right hand side of the same equations). The location of the stability curve at the edge of the loaded area, 75 psi., can also be read directly from Figure 7, employing the co-ordinates $c = 6.9$ psi. and $\theta = 25^\circ$, or

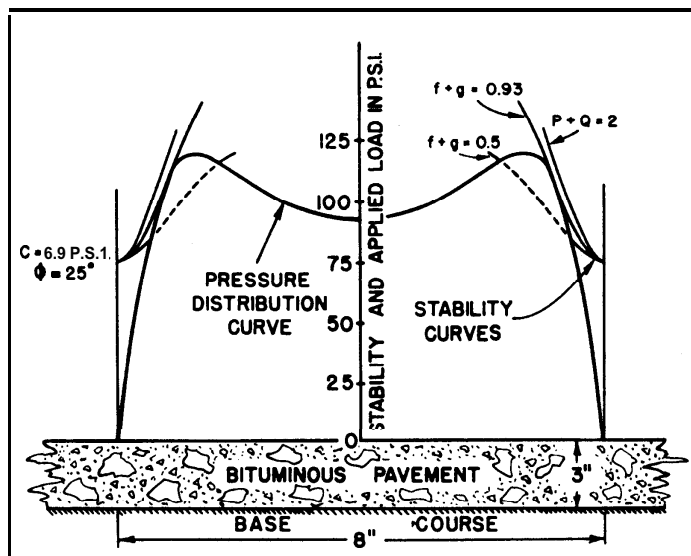


Fig. 13. Influence of Typical Pressure Distribution over the Contact Area, and of Various Degrees of Frictional Resistance Between Pavement and Tire and Between Pavement and Base in Terms of $f + g$ Values on the Design of the Underlying Bituminous Pavement (Truck Tire).

can be calculated by means of equation (3). The increase in stability with increasing distance inward from the edge of the contact area indicated by the stability curves of Figure 13 is due to the frictional resistance between pavement and tire and between pavement and base, and is calculated by means of the third term on the right hand side of equations (10) or (16) and (11) or (17), equations (10) or (16) being employed for the $P + Q = 2$ curve and equations (11) or (17) for the $f + g = 0.93$ and $f + g = 0.5$ curves. These stability curves indicate that because of the influence of these two frictional resistances, the pavement can sustain a higher and higher vertical load as the centre of the contact area is approached from the edge; that is, its stability increases with increasing distance inward from the edge of the loaded area.

The ordinate axis in the centre of the diagram indicates values for both tire pressure exerted on the contact area and pavement stability. If it is assumed that the stability of the pavement must be not less than the pressure applied by the tire at any location on the contact area, then it is apparent that the stability curve must not cut through the pressure curve at any point. It is equally clear that the critical stability curve is the one that is just tangent to the pressure curve. In Figure 13, the stability curve for $f + g = 0.5$ cuts through the pressure curve, indicating that the pavement would be unstable for the portion of the contact area for

which the stability curve lies below the pressure curve. The stability curve for $f + g = 0.93$ is just tangent to the pressure curve, and indicates the lowest value of $f + g$ for which this particular paving mixture ($c = 6.95$ psi., $\phi = 25^\circ$) would be stable at all points on the contact area. The stability curve labelled $P + Q = 2$, on the other hand, indicates the highest $f + g$ values that could be developed for this paving mixture, since any $f + g$ stability curve lying above this $P + Q = 2$ curve would represent a value of frictional resistance between pavement and tire or between pavement and base, or both, that was greater than the shearing resistance of the bituminous pavement. It is apparent that the pavement would fail in shear before such a high value for f or g or $f + g$ could be developed.

The importance of frictional resistance between pavement and tire and between pavement and base on bituminous pavement design is emphasized in Figure 14, in which stability curves for $f + g = 0$, $f + g = 0.2$, $f + g = 0.6$, and $f + g = 1.2$ are shown on the right-hand side. These stability curves demonstrate very clearly the decrease in values of c and ϕ that is possible as the $f + g$ values are increased. For example, when $f + g = 0$, a paving mixture with $c = 7.8$ psi. and $\phi = 30^\circ$ developing a stability of 107 psi. at the edge of the contact area is required, while for $f + g = 1.2$ a bituminous mixture with $c = 4.0$ psi. and $\phi = 30^\circ$ developing a

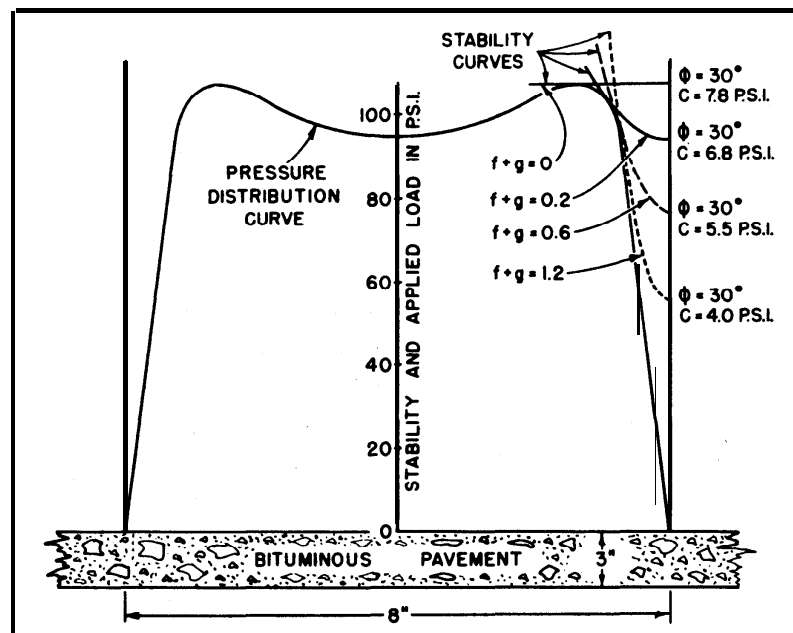


Fig. 14. Illustrating the Influence of Frictional Resistance Between Pavement and Tire and Between Pavement and Base on the Design of Bituminous Pavements.

stability of only 54 psi. at the edge of the contact area is adequate; that is, by increasing the $f + g$ value from 0 to 1.2, the stability requirements for the paving mixture in terms of c and ϕ values have been reduced by one-half.

It has long been known that the stability of a bituminous pavement is materially influenced by its thickness. It has been quite commonly observed that a thick layer of a given bituminous paving mixture may develop instability under either stationary or moving traffic, whereas a thin layer of the same paving mixture may be quite stable under the same traffic. That this is precisely what would be expected if pavement stability is influenced by the frictional resistances between pavement and tire and between pavement and base is illustrated by Figures 15 and 16.

In Figure 15, the pressure curve represents smoothed out data for the variable tire pressure across the transverse axis of the contact area for a load of 200,000 lbs. on a single airplane tire as measured by Porter (5). The stability curves in the upper right-hand corner for different thicknesses of a given bituminous paving mixture ($c = 7.7$ psi., $\phi = 24^\circ$) are based upon equations (11) and (17). Values of $K = 1$ and $f + g = 0.2$ were selected for purposes

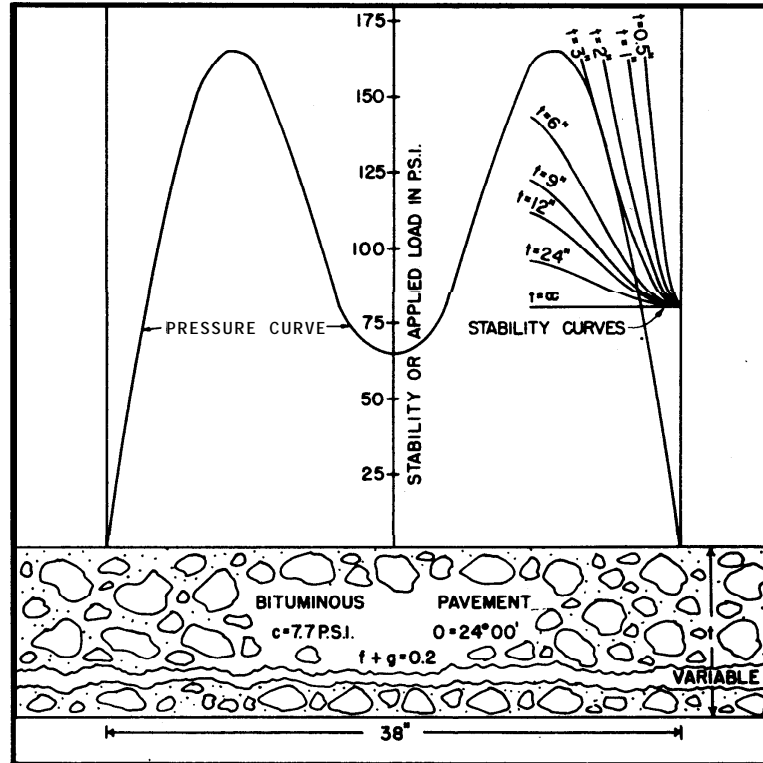


Fig. 15, Influence of Pavement Thickness on Pavement Stability for Stationary Wheel Loads or Wheel Loads Moving at a Uniform Speed (Aeroplane Tire).

of illustration. The value of the thickness t shown for each stability curve can be verified by means of the equations given in Figures 9 or 10, or by equation (17). Figure 15 demonstrates that the maximum thickness of pavement that can be selected for the conditions pertaining to this diagram is 3 in. The stability curve for a thickness of 6 in., for example, cuts through the curve representing applied pressure, and indicates that for this thickness the applied pressure **would** be greater than the pavement stability over a considerable portion of the contact area.

It should be emphasized that the information illustrated in Figure 15 is based entirely upon the pressure distribution curve, paving mixture ($c = 7.7$ psi., $\phi = 24^\circ$), $f + g = 0.2$, $K = 1$, and other conditions illustrated in this figure. A change in any one of these variables would ordinarily have the result that some other thickness than 3 inches would be critical. This is well illustrated in Figure 16, where the pressure distribution curve is for a truck tire, $f + g = 0.6$, $K = 1$, and the characteristics of the paving mixture are represented by $c = 4.54$ psi., $\phi = 29^\circ$. The stability curves in the upper right-hand corner indicate that the stability curve for thickness $t = 1.5$ in. is just tangent to the pressure curve, and is the maximum thickness that could be selected for a stable pavement in this case. If a greater pavement thickness than 1.5 inches

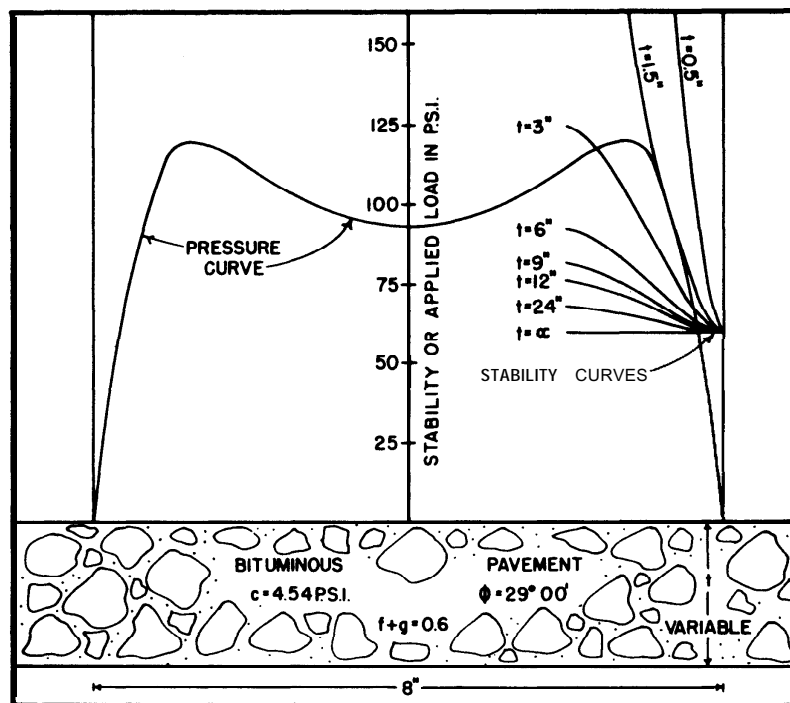


Fig. 16. Influence of Pavement Thickness on Pavement Stability for Stationary Wheel Loads or Wheel Loads Moving at a Uniform Speed (Truck Tire).

were required, it would be necessary to employ a more stable paving mixture (higher values for c or ϕ , or both), or to otherwise modify the conditions represented by Figure 16.

It should be noted again that the influence of pavement thickness on pavement stability indicated by equations (10), (11), (16), and (17), and illustrated in Figures 15 and 16, is in keeping with practical observations of pavement performance under traffic.

In the field of airport runway design, one of the important current problems is presented by the increased tire pressures for landing wheels. Figure 17 demonstrates that on the basis of present tire designs, as the tire pressure is increased, the stability of the paving mixture must be increased. The solid pressure curve in Figure 17 is for an average tire pressure of 100 psi., while the dashed pressure curve corresponds to an average tire pressure of 200 psi., the total wheel load being 8,000 lbs. in each case. If $f + g = 1.0$ in both cases, the stability curves of Figure 17 indicate that the values of c and ϕ must be increased from $c = 4.5$ psi. and $\phi = 30^\circ$, to $c = 9.0$ psi. and $\phi = 30^\circ$, to give approximately double the pavement stability as the tire pressure is increased from 100 psi. to 200 psi. This demonstrates that many existing bituminous pavements will be unstable if tire pressures are increased to 300, 400, 500 psi., etc., as sometimes suggested for future aircraft. In addition, as these tire pressures increase, the c and ϕ values

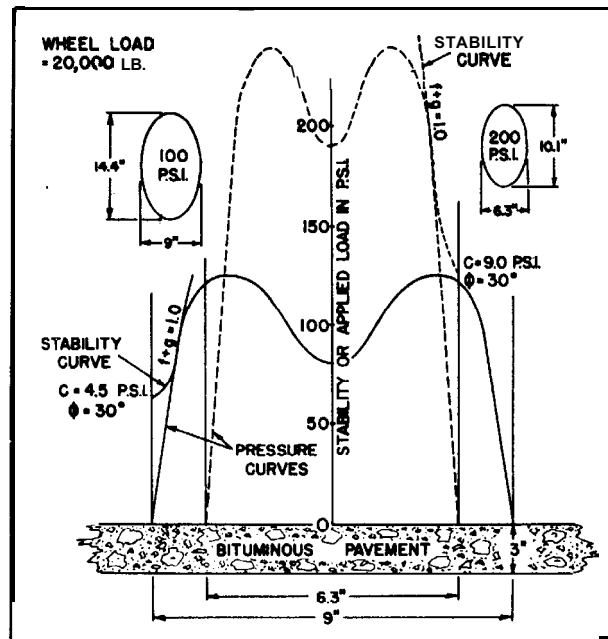


Fig. 17. Illustrating Increased Pavement Stability Required when Tire Pressure Is Increased from 100 to 200 psi.

of paving mixtures must be further increased to provide the necessary pavement stability. This, in turn, means that fewer and fewer aggregates will have the properties needed to produce bituminous pavements with the increased stability required. Furthermore, the design of stable bituminous pavements for these proposed high tire pressures might be a serious problem in areas where only inferior aggregates occur.

On the basis of the subject matter that has just been presented, a rational method of design for bituminous pavements requires that:

- (a) the shape of the most critical curve of distribution of tire pressure on the contact area must be known;
- (b) the coefficients of friction between pavement and tire, f , and between pavement and base, g , must be known;
- (c) values for c and ϕ for the bituminous mixture must be determined;
- (d) the pavement thickness must be specified;
- (e) the stability curve must be drawn using equations (10), (11), (16), or (17); and
- (f) the stability curve should be tangent to or above the pressure distribution curve for all points on the contact area, to provide the minimum stability required.

The Influence of Tire Design

On the basis of Figure 17, if the tire pressure is increased, the stability of the paving mixtures that are to carry these higher tire pressures must also be increased. This is the only solution to the problem of pavement design for higher tire pressures that can be offered by the current empirical methods for bituminous mixture design, such as Hubbard-Field, Hveem, Marshall, etc.

On the other hand, while the rational approach to the design of bituminous paving mixtures that has just been outlined indicates that paving mixtures of greater stability is one answer to the problem of higher tire pressures, it also suggests another possible solution.

Instead of constructing pavements of higher and higher stability, it indicates that by certain modifications in the design of tires, many existing pavements might continue to be stable in spite of much higher tire pressures. In addition, these high tire pressures might be safely carried by new pavements of moderate stability.

The objective to be achieved by the modifications in tire design suggested by this rational approach consists of flattening the slope of the curve of tire pressure distribution near the edge of the

contact area, as illustrated in Figure 18. The unbroken tire pressure distribution curve shown in Figure 18 is representative of that for an average current tire, and has a steep slope near the edge of the contact area. The dashed tire pressure distribution curve illustrates the much flatter slope near the edge of the loaded area that would be obtained by means of a modified tire design. The stability curves tangent to these two pressure distribution curves demonstrate the large decrease in pavement stability (c and ϕ values) that is possible by decreasing the slope of the tire pressure curve near the edge of the contact area. Both stability curves are drawn for a value of $f + g = 0.65$. The stability curve tangent to the steeper unbroken tire pressure curve indicates that a bituminous pavement for which $c = 7.35$ psi. and $\phi = 25^\circ$, providing a stability of 80 psi. (equation 3) at the edge of the contact area (due to the pavement surrounding the loaded area) is required, while the stability curve tangent to the dashed line pressure curve of flatter slope demonstrates that a bituminous pavement for which $c = 1.75$ psi. and $\phi = 25^\circ$, providing a stability of only 19 psi. at the edge of the contact area, is needed; that is, by decreasing the slope of the tire pressure curve near the edge of the contact area (Figure 18), the stability requirement for the paving mixture in this particular case was reduced from 80 psi. to 19 psi.

It is apparent, therefore, that by flattening the slope of the tire pressure distribution curve near the edge of the contact area, very

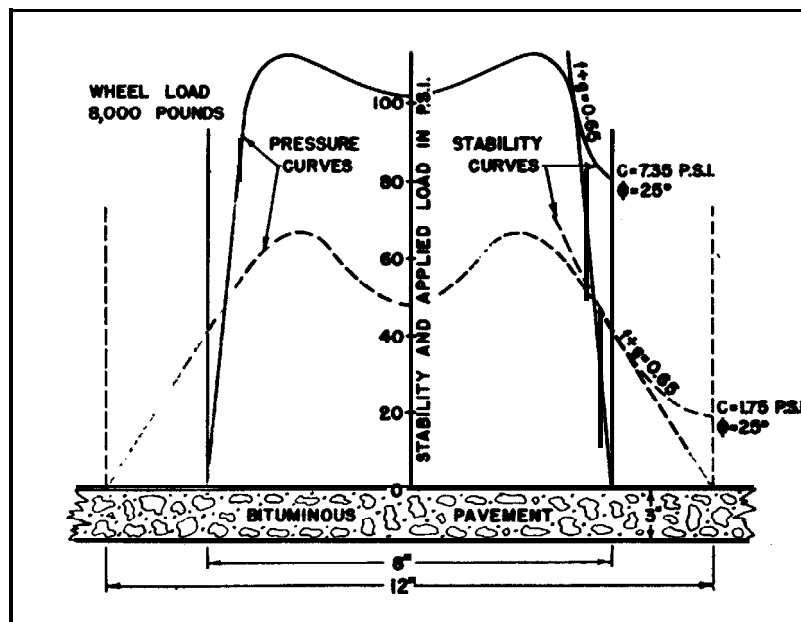


Fig. 18. Influence of Shape of Pressure Distribution Curve Across the Contact Area on Bituminous Pavement Design.

much higher tire pressures could be supported by many existing bituminous pavements, or by new pavements of relatively low stability (low c and ϕ values).

Tire manufacturers may be able to produce ordinary tires for which the slope of the pressure distribution curve is much flatter near the edge of the contact area than is the case with present tires. However, Figure 19 demonstrates that there is more positive approach to this problem, by utilizing a tire containing two or more compartments, more or less concentric, each inflated to a different pressure. Figure 19(a) illustrates such a tire consisting of three compartments inflated to 100, 200, and 400 psi., from outermost to innermost compartments, respectively. Figure 19(b) indicates the action of such a tire when loaded, while Figure 19(c) shows the principal pressure contours on the contact area of this tire. Other pressures could be employed for the compartments than those shown in Figure 19, and it should be clear that many variations of this principle are possible, in some of which rubber of different hardness or softness, etc., might replace one or more of the gas-filled compartments of the tire.

The multi-compartment type of tire illustrated in Figure 19 has two important advantages over existing single compartment tires designed to carry the same total load on the same contact area:

- (a) the flatter slope of the pressure distribution curve near the edge of the contact area lowers the c and ϕ values (stability requirements) needed for a stable paving mixture,
- (b) the applied pressure is higher towards the centre of the contact area, where Figures 11 to 18 have already demonstrated the greatest pavement stability seems to be developed.

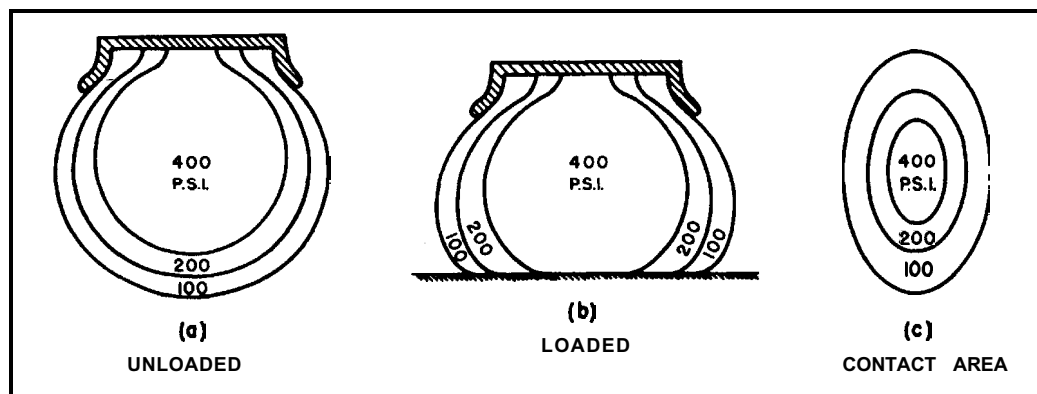


Fig. 19. Diagram of Multi-Compartment Tire.

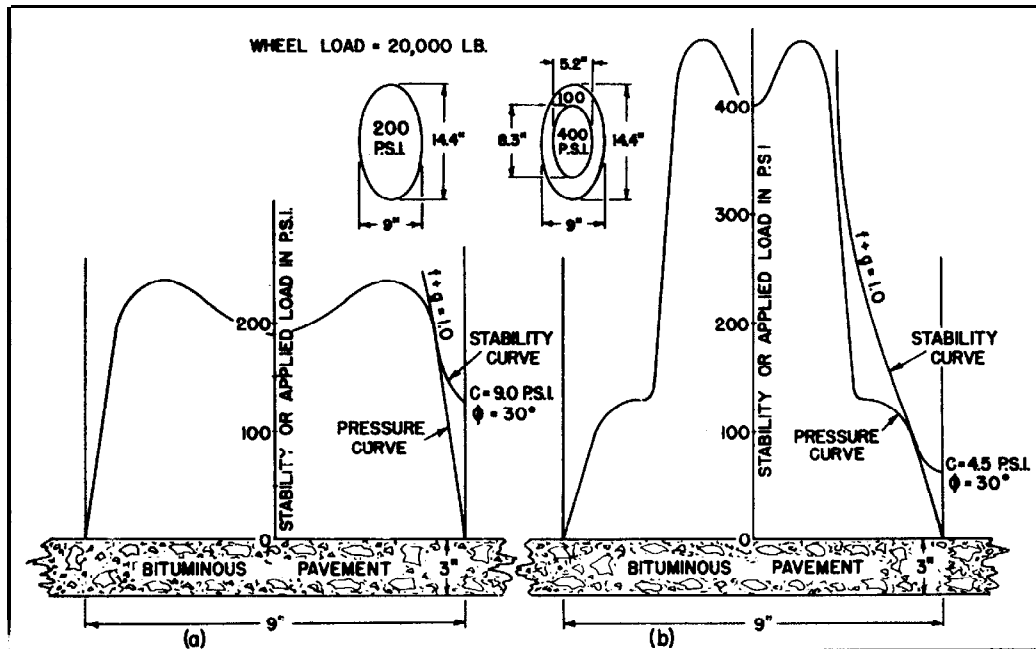


Fig. 20. Illustrating Influence of Tire Design on the Design of Bituminous Pavements for a Wheel Load of 20,000 Pounds.

Figure 20 illustrates the advantage of a two-compartment versus a single compartment tire for a wheel load of 20,000 pounds. The contact areas for both tires are exactly the same. The stability curve in Figure 20(a) that is just tangent to the pressure distribution curve for a single compartment tire inflated to about 200 psi., indicates that a bituminous paving mixture would be required for which $c = 9$ psi. and $\phi = 30^\circ$, developing a stability of about 125 psi. at the edge of the contact area (due to the lateral support of the pavement surrounding the loaded area, equation (3)). Figure 20(b) illustrates a two-compartment tire inflated to 100 psi. in the outer compartment and to 400 psi. in the inner compartment. Because of the overall flattening of the slope of the pressure curve near the edge of the contact area, the stability curve in Figure 20(b) indicates that a bituminous paving mixture would be required for which $c = 4.5$ psi. and $\phi = 30^\circ$, and developing a stability of only about 62 psi. at the edge of the contact area (due to the lateral support of the portion of the pavement surrounding the loaded area, equation (3)). For both Figure 20(a) and Figure 20(b), the stability curves are based upon $f + g = 1.0$. Figure 20 demonstrates, therefore, that by going from a single compartment to a two-compartment tire, the stability of the paving mixture required to carry a wheel load of 20,000 pounds on the contact area shown might be reduced to about one-half; e.g., from about 125 psi. to about 62 psi.

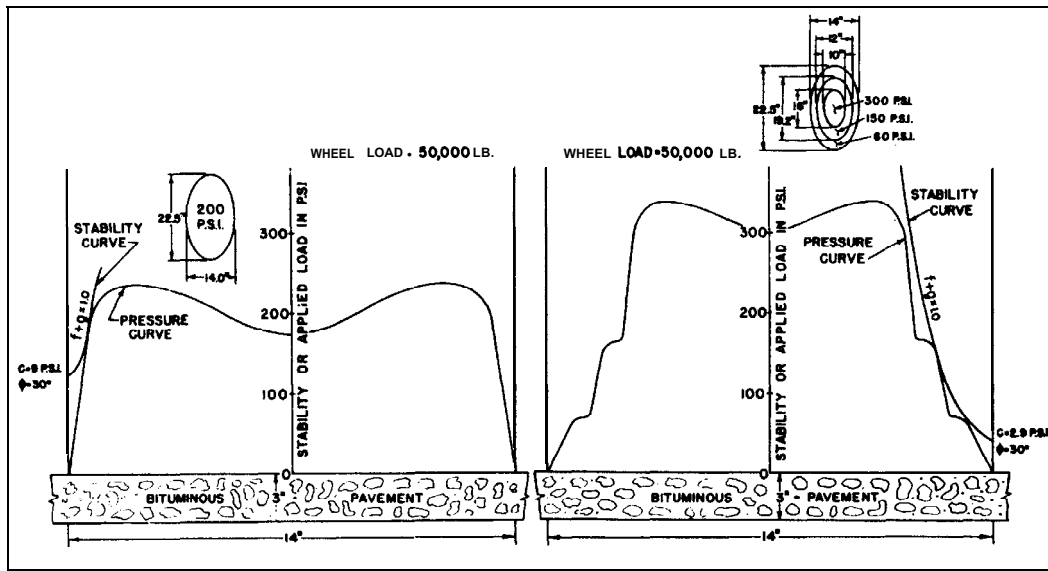


Fig. 21. Illustrating Influence of Tire Design on the Design of Bituminous Pavements for a Wheel Load of 50,000 Pounds.

Figure 21 illustrates the reduction in the stability requirements for the bituminous pavement that is possible for supporting a wheel load of 50,000 pounds on a given contact area, when a triple compartment tire inflated to 60 psi. in the outer compartment, to 150 psi. in the intermediate compartment, and to 300 psi. in the inner compartment, is substituted for a single compartment tire inflated to 200 psi. The stability curve for Figure 21(a) shows that for the single compartment tire a bituminous pavement for which $c = 9$ psi. and $\phi = 30^\circ$, and developing a stability of about 125 psi. at the edge of the contact area (equation (3)) is required. On the other hand, the stability curve for Figure 21(b) indicates that with a triple compartment tire inflated as shown, the same total load could be carried on the same contact area by a bituminous pavement for which $c = 2.9$ psi. and $\phi = 30^\circ$, and which develops a stability of only about 41 psi. at the edge of the contact area. In this case, by substituting a triple compartment tire for the single compartment tire, a reduction of about two-thirds in the stability requirement for the bituminous paving mixture might be made.

Figures 18, 20, and 21 suggest that by flattening the slope of the curve of pressure distribution near the edge of the contact area, many existing bituminous pavements might continue to be stable, even if the average tire pressure were greatly increased above present values. Furthermore, by this modification in tire design, it appears that bituminous pavements with relatively low

c and ϕ values could be designed and constructed that would have quite adequate stability under average tire pressures of several hundred psi.

Comments and Qualifications

1. The rational approach to the design of bituminous pavements that has just been described is based entirely on stress factors, and no direct mention has been made of the strains developed in a pavement subjected to these stresses. Very little information is available concerning the magnitude of the strains a bituminous pavement can withstand without damage. If either the Hveem Stabilometer method, or the Smith triaxial method described in The Asphalt Institute's (10) hot-mix manual, actually subject test specimens to failure conditions as usually claimed for them, the strain at which the failure stress occurs cannot be very large.

It is significant also that in both of these tests (Hveem Stabilometer and Smith triaxial) lateral pressure is measured by the testing equipment for very small vertical pressures on the test specimens. This seems to indicate that the prism of pavement immediately beneath the loaded area is able to develop lateral support from the adjacent pavement under wheel loads and tire pressures that are only a fraction of the pavement's ultimate bearing capacity.

It is clear that some strain must be developed in the portion of the pavement immediately under the loaded area, before it can begin to mobilize lateral support from the adjacent pavement. Also, some strain must occur before the pavement can develop the frictional resistances between pavement and tire and between pavement and base.. That repeated strains of some magnitude under traffic loads are beneficial to bituminous pavements rather than detrimental is indicated by the often repeated and thoroughly substantiated statement to the effect that bituminous pavements require the kneading action of traffic to keep them in good condition.

It is common practice in North America to measure the strength of test specimens of bituminous mixtures at 140°F., which is frequently quoted as the maximum pavement temperature developed under the summer sun on this continent. Consequently, if the pavement is sufficiently stable to support traffic loads when its temperature is 140°F., it has a large safety factor at much lower temperatures as far as strength is concerned. However, more information must be obtained before

it can be determined what factor of safety should be selected for both stress and strain under service conditions at the critical temperature of 140°F.

It should be noted that all present design methods, Hubbard-Field, Marshall, Hveem, and triaxial, test specimens of bituminous mixtures to failure and report stability at failure as the strength of the mixture. If the strain corresponding to the failure stress is greater than could be permitted for a pavement under traffic loads, any factor of safety with respect to strain which is being unwittingly introduced into the actual design and construction of bituminous pavements at the present time is also effective with respect to stress, and vice versa.

Consideration of a maximum permissible strain less than that corresponding to failure conditions would not eliminate any of the stress items on which the rational method of design outlined here is based, but would have the effect of applying a factor of safety to each of them.

2. It should be carefully noted that the possible advantages of a multi-compartment tire for simplifying pavement design for high tire pressures are dependent upon the fact that frictional resistance between pavement and tire and between pavement and base appears to be an important source of pavement stability. If due to considerations of limited permissible maximum strain within the pavement under service conditions, it should be necessary to apply an appreciable factor of safety to these two frictional resistances, the advantages of a multi-compartment over a single compartment tire would be reduced, and if this factor of safety were large enough, these advantages would disappear insofar as their being of any practical value is concerned.
3. It has been assumed in the foregoing section of this paper that the underlying base course would not fail in shear at any point under whatever wheel load was applied to the pavement surface. It should be pointed out, however, that if the shearing resistance of the base course should be less than that of the asphalt surface, the maximum coefficient of friction g that could be developed between asphalt pavement and base would depend upon the shearing resistance of the base course rather than the shearing resistance of the asphalt surface. In addition, the factor Q would refer to the shearing resistance of the base course rather than shearing resistance of the asphalt pavement.
4. While it was assumed at the beginning of this paper that the base course would not fail under the shearing stresses imposed

by any load applied at the surface of the bituminous pavement, it should be pointed out that the pressure applied by the innermost compartment of a multi-compartment tire may be quite high, e.g., Figure 20(b), and that it may be the cause of very high shearing stresses in the underlying base course. This may also be true of a high pressure single compartment tire, e.g., Figure 20(a). Consequently, in actual design, two criteria of failure must be investigated, (a) the tendency of the bituminous pavement to be squeezed out between the tire and the base course, and (b) the tendency of failure to occur along some failure curve extending into the base, e.g., Figure 22. The first of these two criteria of failure has been considered in this paper, and some reference to the second has been made elsewhere (11) in connection with vehicle mobility over a layer of soft soil.

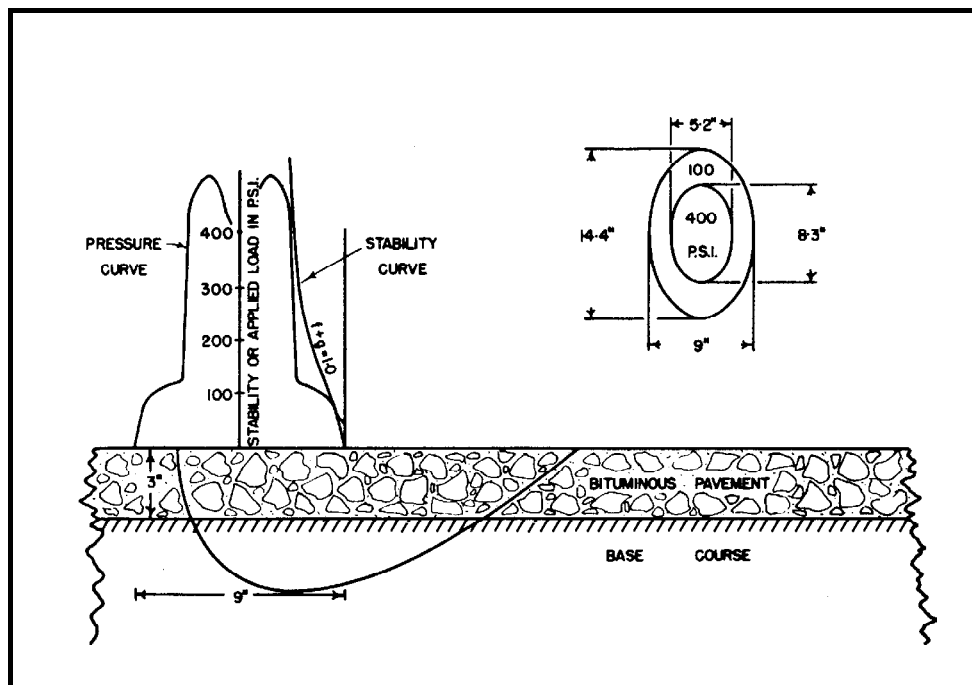


Fig. 22. Illustrating Failure by Squeezing Out the Asphalt Pavement Between Tire and Base Course Versus Failure Along a Logarithm c Spiral Curve Through Pavement and Base.

5. It is realized that the design and manufacture of the **multi-compartment** tires referred to in this paper may present several practical problems, which, however, should not be insurmountable. Nevertheless, regardless of these practical difficulties, it has been one of the objectives of this paper to

demonstrate that the application of several well-known principles of soil mechanics to certain problems in the field of bituminous pavement design appears to point directly to the multi-compartment tire or its equivalent as a possible useful solution.

It has been pointed out elsewhere (11), that the multi-compartment tire may also provide a useful approach to the solution of certain problems in vehicle mobility and soil compaction.

6. It is worth noting that regardless of what the practicability of the multi-compartment tire may be as a solution to the difficulties of designing bituminous pavements of sufficient stability for high tire pressures, it represents an answer to this problem that would not even be dreamed about as long as empirical tests such as Hubbard-Field, Hveem, Marshall, etc., are the sole approach employed for bituminous paving mixture design. As in any other engineering field, therefore, one of the important advantages that would accrue from the development of a rational method of design for the stability of bituminous pavements, would be the greatly widened horizon of availability of possible solutions for the various practical problems that have to be solved.

BITUMINOUS MIXTURES WITH CURVED MOHR ENVELOPES

The previous section of this paper has dealt with the rational design of bituminous paving mixtures with straight line Mohr envelopes. While the limited test data available seem to indicate that straight line Mohr envelopes result from the triaxial testing of the majority of bituminous mixtures, there are indications that for some bituminous mixtures the triaxial data plot as curved Mohr envelopes. If a rational method of design for bituminous paving mixtures is to be developed, it should apply to those with curved as well as to those with straight Mohr envelopes.

Not enough appears to be known about the triaxial testing of bituminous mixtures to establish why straight line Mohr envelopes are obtained for some and curved Mohr envelopes for others. It will be assumed in this paper that either type of Mohr envelope may occur for quite valid, although presently uncertain, fundamental reasons, and that the difference is not due to certain easily controllable variables such as inadequate compaction during the preparation of the test specimens, improper dimensions of the test specimen, etc.

It should be observed in this connection that the Mohr theory

does not require that the Mohr envelope be a straight line (12). It leaves the shape of the Mohr envelope to be established by experimental data. Consequently, the Mohr envelope may be either a straight line or curved, depending upon the test data.

In the earlier part of this paper, in which straight line Mohr envelopes were assumed, the further assumption was made that the point of tangency between any Mohr circle and the Mohr envelope defined the angle of the plane of failure through the test specimen, Figures 3 and 5, and that this angle of failure, $45 - \frac{\phi}{2}$, from the vertical, Figure 5, was constant regardless of the magnitude of the principal stresses V and L applied to the specimen under failure conditions.

In the paper by Hennes and Wang (13) presented at last year's meeting, consideration was given to the nature of the Mohr diagram for tests on materials that are not isotropic; that is, materials for which the shearing strength varies for different planes through the test specimen. Their paper mentioned the earlier studies of the strength of non-isotropic materials by Carillo and Casagrande (14), and by Hank and McCarty (15). Reference should also be made to the valuable discussions by Barber following the papers by Hank and McCarty and by Hennes and Wang.

For the conditions of non-isotropy mentioned by Hennes and Wang (different shearing strengths on major and minor principal planes through the test specimen), the Mohr circles resulting from both a hypothetical study and actual triaxial data were such that a common straight line tangent could be drawn. However, the point of contact between tangent and circle in this case did not define the angle of the plane of failure through the specimen, and this conclusion should be kept in mind when testing specimens which may not be isotropic, and for which the straight line tangent may be erroneously taken to be a straight line Mohr envelope.

Nevertheless, the paper by Hennes and Wang illustrates the **fact** that Mohr circles for non-isotropic materials may have a common straight line tangent and indicates further that lack of isotropy in itself does not necessarily result in Mohr circles having a curved Mohr envelope. Consequently, for the balance of this paper, it is assumed that curved Mohr envelopes result from the triaxial testing of certain bituminous paving mixtures, and that the curvature of the Mohr envelope is a fundamental and not accidental characteristic of these mixtures. To simplify the presentation, the further simplifying assumption is made that the point of contact between the curved Mohr envelope and any Mohr circle defines the angle of the plane of failure through the specimen for

the particular conditions of stress represented by that Mohr circle.

Figure 23 illustrates the curved line relationship of the principal stress diagram, Figure 23(b), that may result from the plotting of triaxial data for certain bituminous paving mixtures, and the curved line Mohr envelope in the corresponding Mohr diagram, Figure 23(c).

The first decision to be made by the design engineer, when he finds that the triaxial data result in a curved line relationship between the principal stresses, is whether the degree of curvature is so great that a serious error in design might occur if he neglected the curvature, drew the best straight line through the data, which in turn would result in a straight line Mohr envelope, and then handled the design problem as outlined in the first part of this paper, or by some similar approach. His decision in this

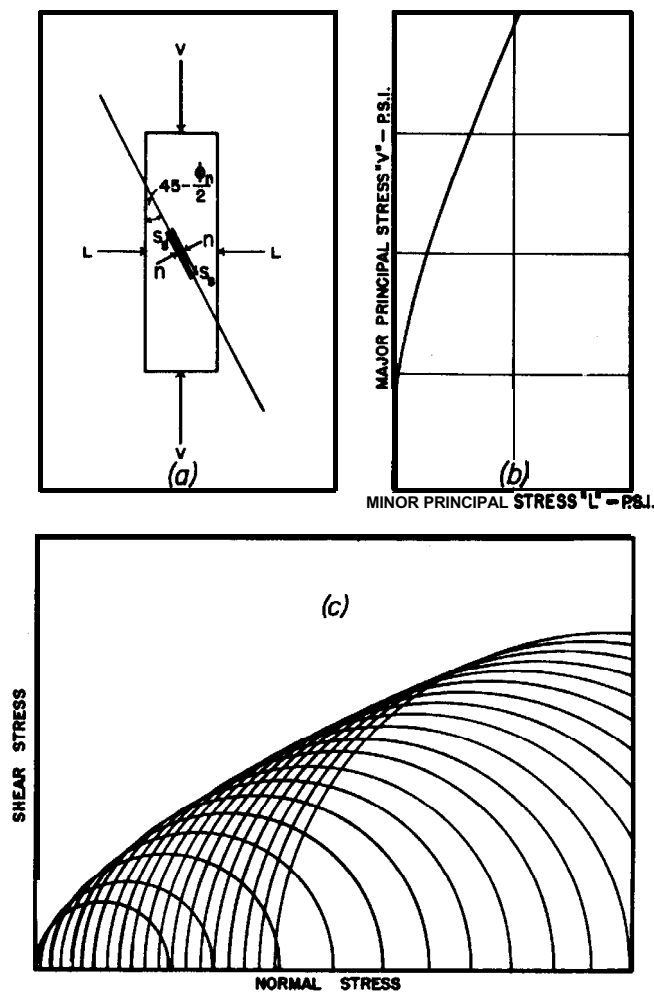


Fig. 23. Corresponding Principal Stress and Mohr Diagrams that Result in a Curved Mohr Envelope.

respect should depend upon the margin of error that might occur through this neglect to handle the problem of design on the basis of a curved line Mohr envelope. For this reason, it is necessary for comparative purposes to have a method of design based upon a curved Mohr envelope corresponding to that outlined in the first part of this paper for a straight Mohr envelope. This is the principal objective of the second part of the present paper.

Figure 24 demonstrates two important differences between Mohr diagrams with curved Mohr envelopes, and those with straight Mohr envelopes. As previously pointed out, it is assumed throughout this paper that the point of tangency between a Mohr circle, and the Mohr envelope tangent to it, defines the angle of the plane of failure through the test specimen. The angle of the plane of failure, frequently designated by θ , is equal to $45 - \frac{\phi}{2}$.

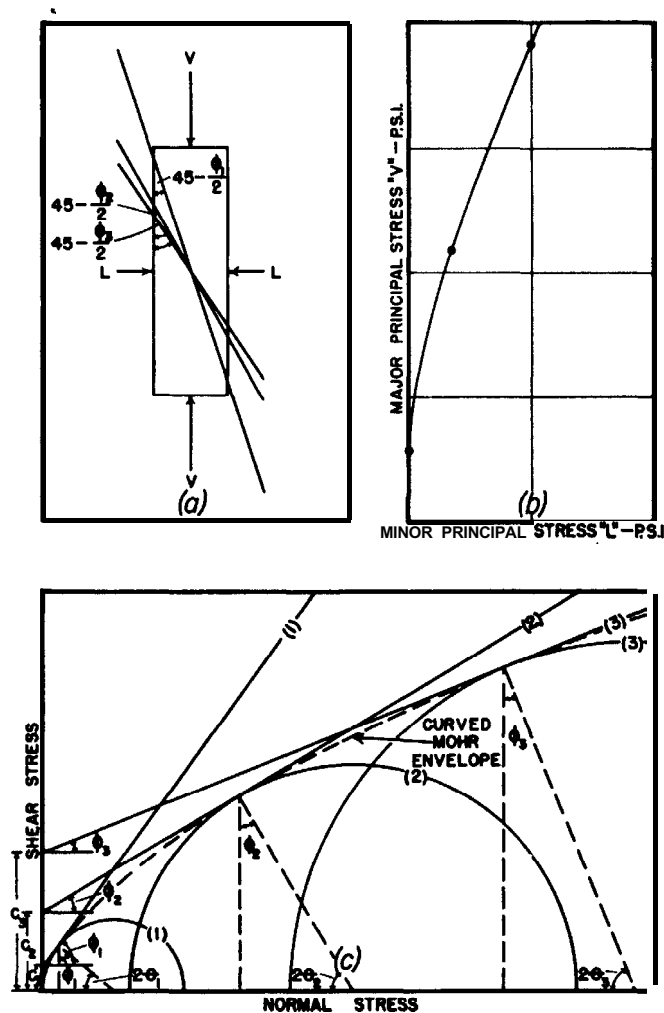


Fig. 24. An Interpretation of the Significance of Curved Mohr Envelopes.

For any given straight line Mohr envelope, the value of θ is constant for all Mohr circles to which it is tangent. Figure 24(c) shows that for a curved Mohr envelope, on the other hand, the value of θ is different for every Mohr circle. It is smallest for the Mohr circle representing the unconfined compressive strength (extreme left of Figure 24(c)), and becomes gradually larger for Mohr circles corresponding to successively greater magnitudes of the principal stresses V and L acting on the test specimen under incipient failure conditions (proceeding toward the right in Figure 24(c)). This is further illustrated in Figure 24(a). This means that for materials with curved Mohr envelopes, the angle of the plane of failure through the test specimen is not constant, but varies with the magnitude of the principal stresses to which the test specimen is subjected at failure. Theoretically at least, it appears that as the magnitude of the principal stresses is increased, the angle-of the plane of failure through the test specimen, θ , approaches an asymptotic value of 45° , and that correspondingly the angle of internal friction ϕ approaches 0° as an asymptote.

The second important difference between Mohr diagrams for straight versus curved Mohr envelopes concerns the values of cohesion c and angle of internal friction ϕ . When the Mohr envelope is straight, Figure 3, the Mohr diagram shows that there is only one value for cohesion c and angle of internal friction ϕ for the material, regardless of the magnitudes of the corresponding principal stresses V and L applied to the test specimen. However, for Mohr diagrams for which the Mohr envelope is curved, Figure 24(c) demonstrates that if the tangent to a Mohr circle at its point of tangency with the curved Mohr envelope represents the values of c and ϕ to be associated with that Mohr circle, then the values of c and ϕ for the material vary from Mohr circle to Mohr circle throughout the Mohr diagram, and are, therefore, dependent upon the magnitude of the corresponding values of the principal stresses V and L applied to the test specimen under conditions of incipient failure. Consequently, as shown in Figure 24(c), the values of cohesion c and of angle of internal friction ϕ associated with Mohr circle (1) are c_1 and ϕ_1 , with Mohr circle (2) are c_2 and ϕ_2 , with Mohr circle (3) are c_3 and ϕ_3 , etc.

Equations (9), (10), (11), (16), and (17), previously given, are expressed in terms of cohesion c and angle of internal friction ϕ . Since they were developed for a straight line Mohr envelope, the values for c and ϕ were constant and could be applied to any Mohr circle throughout the Mohr diagram. If these same or similar equations are to be utilized for the design of bituminous paving

mixtures with curved Mohr envelopes, Figure 24(c) indicates that some decision must be made concerning the particular values of c and ϕ to be used for substitution in equations (9), (10), (11), (16), and (17), or modifications of these. Since in this case the values of c and ϕ vary from Mohr circle to Mohr circle throughout the Mohr diagram, it is first of all necessary to establish which Mohr circle represents the most critical conditions of stress to which the paving mixture will be subjected in the field.

In the first part of this paper, it was suggested that the lateral support provided by the portion of the pavement immediately adjacent to the prism of pavement just beneath the contact area could be conservatively taken as being equal to the unconfined compressive strength of the paving mixture. It was pointed out that the magnitude of this lateral support could be expressed exactly as the unconfined compressive strength multiplied by a factor K , where K when evaluated might turn out to be either equal to, greater than, or less than unity. Let it be assumed that the lateral support provided by the pavement adjacent to the loaded prism under the contact area is equal to the unconfined compressive strength of the paving mixture, which is represented by the Mohr circle on the left in Figure 6. If it is also assumed, for the purpose of simplification, that the frictional resistances between pavement and tire and between pavement and base are equal to zero, then the second Mohr circle from the left in Figure 6 represents the conditions of stress to which the prism of pavement immediately beneath the loaded area is subjected under the condition of incipient failure. It is this prism of material that must not fail under the most critical conditions of loading in the field, and that must develop sufficient stability or strength to support the applied load. On the basis of these assumptions, therefore, the values of c and ϕ provided by the tangent to the second Mohr circle from the left in Figure 6, at this circle's point of tangency with the Mohr envelope, are the c and ϕ values to be substituted in equations (9), (10), (11), (16), or (17), to determine the stability or load supporting value of the paving mixture. In the case of a Mohr diagram with a straight Mohr envelope, the values for c and ϕ for this Mohr circle are of course the same as those for any other Mohr circle in the diagram.

Regardless of whether the Mohr envelope is straight or curved, the most critical-Mohr circle is that which represents the most critical conditions of stress for the prism of pavement just beneath the contact area. In Figure 26, where the Mohr envelope is curved, let the simplifying assumption again be made that the frictional resistances between pavement and tire and between

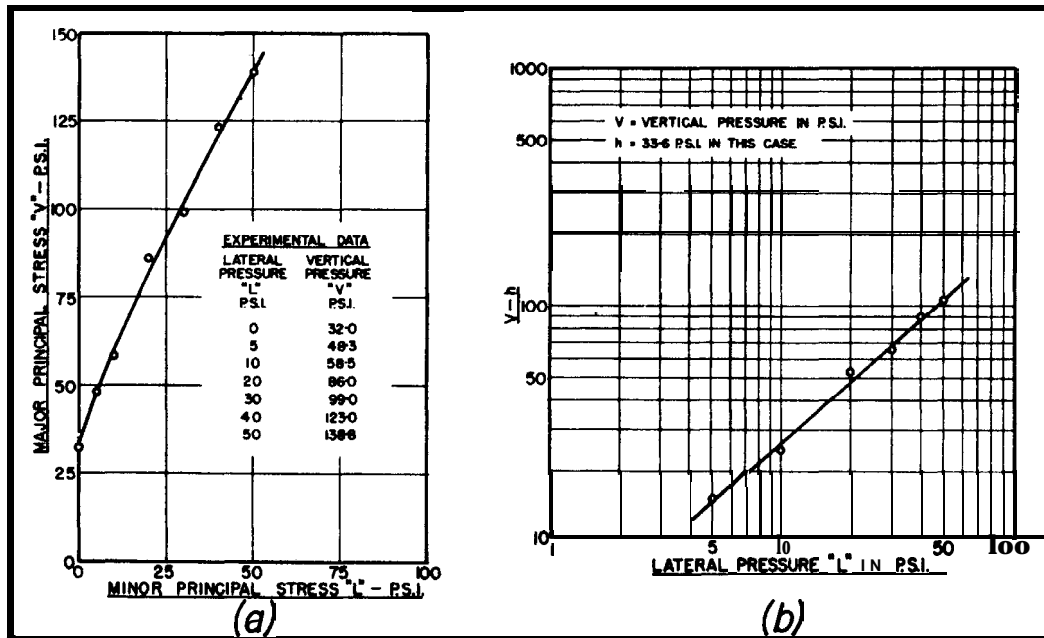


Fig. 25. Procedure for Locating the Best Smooth Curve Through the Points on a Principal Stress Diagram in which the Points Fall along a Curved Rather than a Straight Line.

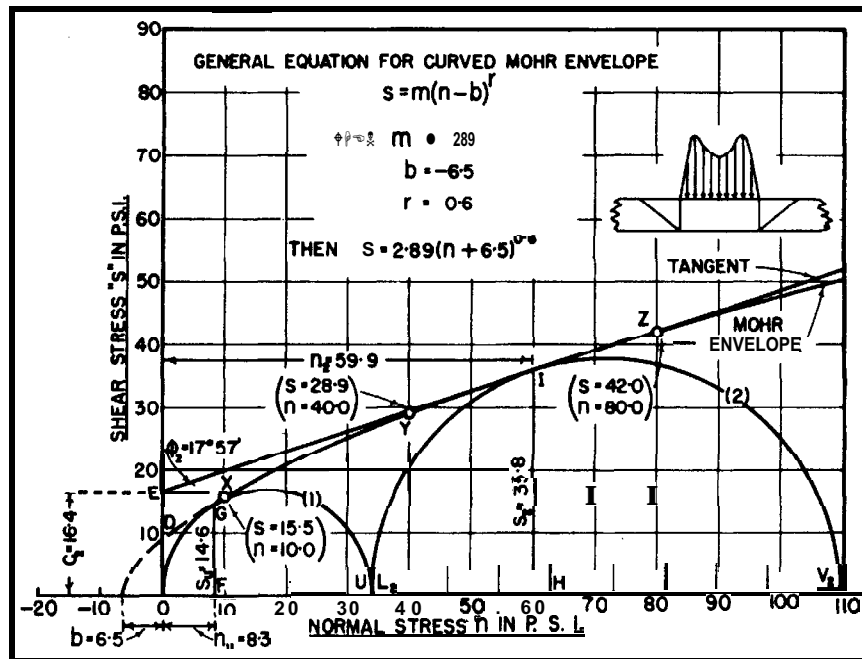


Fig. 26. Illustrating Maximum Vertical Load V Supported by a Bituminous Paving Mixture with a Curved Mohr Envelope when the Lateral Support L Is Equal to the Unconfined Compressive Strength of the Material.

pavement and base are zero, and that the lateral support of the portion of the pavement adjacent to the prism under the loaded area is equal to the unconfined compressive strength of the paving mixture, which is represented by the Mohr circle (1). The conditions of stress for the prism of pavement just under the loaded area are, therefore, represented by Mohr circle (2). Consequently, in Figure 26 the tangent at the point of tangency I between Mohr circle (2) and the curved envelope provides the values of c and ϕ required for substitution in equation (9), and in slight modifications of equations (10), (11), (16), and (17), for calculating the stability or load carrying capacity V of the paving mixture. This also applies in a similar manner to the more general case illustrated by the tangent to Mohr circle (3) in Figure 27, where the lateral support of the loaded area is shown to be equal to the unconfined compressive strength of the paving mixture multiplied by the factor K already described.

In the previous paragraph, it was stated that slight modifications must be made to equations (10), (11), (16), and (17) before they can be employed for the design of bituminous paving mixtures with curved Mohr envelopes. These modifications are necessary

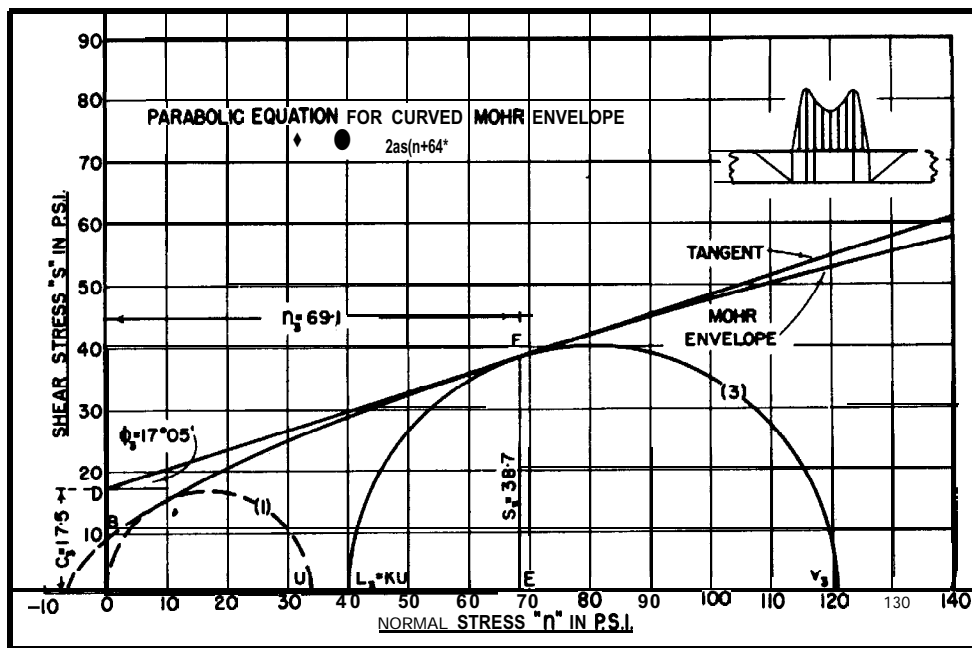


Fig. 27. Illustrating Maximum Vertical Load V that Can Be Carried by a Bituminous Paving Mixture with a Curved Mohr Envelope when the Lateral Support KU Is Either a Fraction or a Multiple of the Unconfined Compressive Strength of the Material (General Case).

because, as Figures 26, 27, and 28 clearly indicate, the values for c and ϕ given by the tangent to the Mohr circle at its point of tangency with the Mohr envelope are different for the Mohr circle on the left representing the unconfined compressive strength, than those for the second Mohr circle from the left corresponding to the critical conditions of stress in the prism of pavement just under the loaded area; that is, instead of one set of c and ϕ values for use in equations (10), (11), (16), and (17), as given by a straight line Mohr envelope, two sets of c and ϕ values or their equivalent must be introduced into these equations, if they are to be employed for materials with curved Mohr envelopes. The modifications of these equations required for this purpose will now be considered.

Equation (9),

$$V = 2c \sqrt{\frac{1 + \sin \phi}{1 - \sin \phi}} + L_S \left(\frac{1 + \sin \phi}{1 - \sin \phi} \right) + L_R \left(\frac{1 + \sin \phi}{1 - \sin \phi} \right) \quad (9),$$

which is the basis for equations (10), (11), (16), and (17), can be employed for the design of bituminous mixtures with either straight or curved Mohr envelopes, provided the significance of each symbol in the terms on the right hand side is kept clearly in mind. When it is to be employed for those with curved envelopes, the principal point to be carefully noted is that every item in each of these terms, except L_S , depends upon the nature of the material

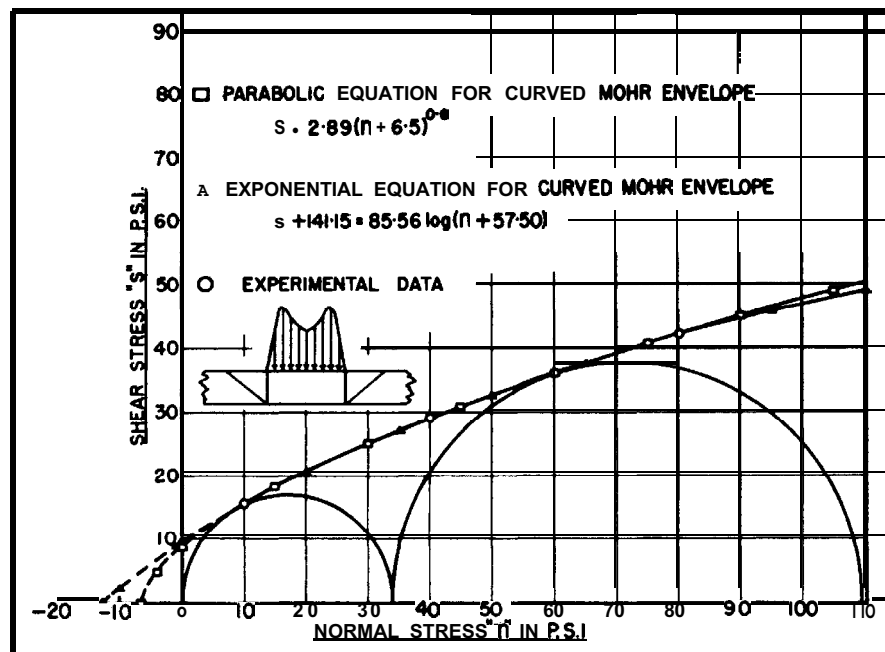


Fig. 28. Illustrating that a Curved Mohr Envelope Can Be Represented by Either a Parabolic or Exponential Equation.

and the conditions of stress in the prism of pavement immediately beneath the contact area, which are assumed for purposes of simplification to be represented by the second Mohr circle from the left in Figures 26 and 27. L_S , on the other hand, refers to the material and the conditions of stress within the pavement surrounding the prism under the loaded area and is represented by the Mohr circle on the left in Figure 26, where L_S is taken to be equal to the unconfined compressive strength of the paving mixture, U , and by the point KU in Figure 27, representing the general case where L_S is considered equal to the unconfined compressive strength multiplied by the factor K .

It is assumed, therefore, that except for L_S , the value of every item or symbol in the three terms on the right hand side of equation (2) is controlled by the conditions of stress within the prism of pavement just under the contact area. Consequently, the values of c and ϕ to be employed when utilizing modifications of equations (10), (11), (16), and (17) for the design of bituminous pavements with curved Mohr envelopes, are given by the tangent to the second Mohr circle from the left in Figures 26 and 27, at its point of tangency with the curved envelope.

With these various points in mind concerning the design of bituminous mixtures with curved Mohr envelopes, equation (10) may be written as

$$V = 2c \sqrt{\frac{1 + \sin \phi}{1 - \sin \phi}} + L_S \left(\frac{1 + \sin \phi}{1 - \sin \phi} \right) + n(P + Q) (c + V' \tan \phi) \left(\tan \left(45 - \frac{\phi}{2} \right) \right) \left(\frac{1 + \sin \phi}{1 - \sin \phi} \right) \quad (18)$$

equation (11) may be written as

$$v = 2c \sqrt{\frac{1 + \sin \phi}{1 - \sin \phi}} + L_S \left(\frac{1 + \sin \phi}{1 - \sin \phi} \right) + n V' (f + g) \left(\tan \left(45 - \frac{\phi}{2} \right) \right) \left(\frac{1 + \sin \phi}{1 - \sin \phi} \right) \quad (19)$$

equation (16) may be written as

$$V = 2c \sqrt{\frac{1 + \sin \phi}{1 - \sin \phi}} + L_S \left(\frac{1 + \sin \phi}{1 - \sin \phi} \right) + \frac{d}{t} (P + Q) (c + V' \tan \phi) \left(\frac{1 + \sin \phi}{1 - \sin \phi} \right) \quad (20)$$

equation (17) may be written as

$$V = 2c \sqrt{\frac{1 + \sin \phi}{1 - \sin \phi}} + L_S \left(\frac{1 + \sin \phi}{1 - \sin \phi} \right) + \frac{d}{t} V' (f + g) \left(\frac{1 + \sin \phi}{1 - \sin \phi} \right) \quad (21)$$

where

the values for c and ϕ are given by the tangent to the second Mohr circle from the left in Figures 26 and 27 at its point of tangency with the curved envelope,

and the value of L_S is given either by the measured unconfined compressive strength of the paving mixture; that is, by the point U in the Mohr diagram of Figure 26, or by the unconfined compressive strength multiplied by the factor K (the general case), as illustrated by the point KU in Figure 27.

While the numerical value to be employed for L_S can be directly read off Mohr diagrams such as those of Figures 26 and 27, and substituted in equations (18), (19), (20), and (21), it is also possible to express L_S in terms of c_u and ϕ_u , where c_u is the value of cohesion c for the unconfined compressive strength given by the tangent to the Mohr circle on the left in Figures 26 or 27 at its point of tangency with the curved envelope, and ϕ_u is the value of the angle of internal friction ϕ given by the same tangent.

In this case, L_S can be expressed by the following equation:

$$L_S = 2c_u K \sqrt{\frac{1 + \sin \phi}{1 - \sin \phi}} \quad (22)$$

where c_u and ϕ_u are the values of cohesion c and angle of internal friction ϕ given by the tangent to the Mohr circle representing the unconfined compressive strength (circle No. 1 in Figures 26 and 27), at its point of tangency with the curved Mohr envelope.

The general similarity of equation (22) for use with a curved Mohr envelope, and of equation (4) employed for a straight Mohr envelope is apparent. Whenever there is any advantage in so doing, equation (22) can be substituted for L_S in equations (18), (19), (20), or (21).

Analysis of Mohr Diagram with a Curved Mohr Envelope

As already indicated, one of the principal problems presented by triaxial data for a bituminous paving mixture that plot as a curved Mohr envelope, is the determination of the values for c and ϕ to be substituted in equations (18), (19), (20), or (21), in order that the stability V of the pavement constructed with the

paving mixture can be calculated by these equations. A method for this purpose, involving a number of successive steps, will be outlined.

Step No. 1

Plot the V and L values from the triaxial data in the form of a principal stress diagram, Figure 25(a). A smooth curve may be drawn through the points arbitrarily. The location of the best smooth curve through the points can be established more accurately, if the V and L data can be plotted as a straight line on some other graph such as log-log, semi-log, etc., by methods available for this purpose (16), Figure 25(b). It happens that the data in Figure 25(a) can be represented by the equation $V = mL^b + h$, in which m , b , and h are constants. This equation provides a straight line on log-log paper when $\log(V - h)$ is plotted versus $\log L$, Figure 25(b). Points from this straight line are transferred back to the principal stress diagram, and a smooth curve is drawn through them, Figure 25(a).

Step No. 2

Transfer several V and L values from the smooth curve of Figure 25(a) to the corresponding Mohr diagram, Figures 26 and 27, and draw the Mohr circles for them. Because of further reference to be made to them, only two of these Mohr circles are retained in Figures 26 and 27, and this procedure is better illustrated by Figures 23 and 24. The values of V and L selected should range from the unconfined compressive strength, $L = 0$, to those large enough to somewhat exceed the probable stability of the paving mixture. This can be roughly estimated by inspection of the resulting Mohr diagrams, e.g., Figures 26, 27, or 28, or of the stability diagram, e.g., Figure 29(c). Draw a smooth curved line envelope tangent to the several Mohr circles, Figures 26 and 27 (better illustrated in Figure 24).

Step No. 3 - Graphical Solution for c and ϕ Values

Mark the Mohr circle representing the unconfined compressive strength, Mohr circle (1) in Figures 26 and 27. The diameter of this Mohr circle is equal to the intercept of the smooth curve on the V axis of Figure 25(a). Mark, also, the Mohr circle for which the unconfined compressive strength U provides the lateral support L_S , Mohr circle (2) in Figure 26. If the lateral support provided by the portion of the pavement adjacent to the loaded area is

equal to the unconfined compressive strength U , then Mohr circle (2) in Figure 26 represents the conditions of stress in the prism of pavement just under the contact area. Therefore, as previously explained, the tangent at the point of tangency I of Mohr circle (2) with the curved envelope provides the required values for c and ϕ to be substituted in the stability equations (18), (19), (20), or (21). The position of this tangent can be estimated visually and drawn in graphically, Figure 26. The required value of ϕ is obtained from the slope of this tangent since the slope is equal to $\tan \phi$, while the value of c is measured by the intercept of the tangent with the shear stress axis. The value of L_S for use in equations (18), (19), (20), and (21) can be read off either as point $L = U$ in Figure 26, or as the intercept of the curve with the V axis in Figure 25(a).

If the lateral support of the portion of the pavement adjacent to the loaded area is considered to be equal to K times the unconfined compressive strength U , where K may be either greater than or less than unity, then Mohr circle (3) in Figure 27 represents the conditions of stress in the prism of pavement just under the contact area (K is illustrated as being greater than unity in Figure 27). In this case, the required values for c and ϕ are again given by the tangent at the point of tangency F of this second Mohr circle with the curved envelope, and can be substituted in equations (18), (19), (20), or (21). The value of L_S to be used in these equations is illustrated by the point $L = KU$ in Figure 27.

The above procedure, therefore, outlines a simple graphical method for obtaining the values of c and ϕ to be used in equations (18), (19), (20), or (21), for determining the stability of bituminous paving mixtures with curved Mohr envelopes.

Step No. 4 - Mathematical Solution for c and ϕ Values

From visual examination of Figures 26 and 27, it is clear that due to the considerable distance over which the curved envelope and Mohr circle circumference are very near to each other, the exact point of tangency between the two, I in Figure 26, and F in Figure 27, is not easily determined by inspection, and some error could also be made in its slope when the tangent is drawn. The graphical method for determining the values of c and ϕ described under Step No. 3 is, therefore, subject to these same errors, plus any additional errors made in measuring the slope of the tangent and its intercept with the shear stress axis. To whatever extent the effect of the magnitude of these errors might be serious when cumulative, it is worth while to have a rigorous mathematical

method for establishing the exact point of tangency between the curved envelope and any Mohr circle, and exact values for c and ϕ for substitution in equations (18), (19), (20), and (21). The balance of this section will be devoted to the outline of a rigorous mathematical method for this purpose, which is presented in detail in the appendix to this paper.

The first step in this development consists of obtaining a relatively simple mathematical equation for the smooth curved Mohr envelope that was drawn under Step No. 2 above. Two simple types of equations available for this purpose are power functions and exponential functions. An equation of the power function type that gives a parabolic curve is $s = m(n - b)^r$, Figures 26, 27, and 28, where m , b , and r are constants, while s = shearing stress and n = normal stress. The exponential function type is illustrated by the equation $s + d = m \log(n + a)$, Figure 28, where d , m , and a are constants, while s = shearing stress and n = normal stress.

Each of these two types of equations contains three unknown constants. In each case, these constants can be evaluated by solving the simultaneous equations that result from substitution of the s and n values for three well-distributed points, e.g., X, Y, and Z in Figure 26, on the smooth curve that is to be represented by a mathematical equation. As indicated by Figure 26, the three points X, Y, and Z should be well distributed over the range from slightly more than the unconfined compressive strength, point X, to somewhat beyond the probable stability of the paving mixture, point Z. In Figure 26, the s and n coordinate values are shown for each of the three points X, Y, and Z, and they should be read as precisely as possible from the smooth curve.

When the constants in both the power and exponential equations have been evaluated in this manner, Figure 28 demonstrates that either type of equation fits the original smoothly-drawn curved Mohr envelope, on which the three points lie, equally well, over the range of stability concerned. At either end of this range, it is seen that the curves provided by the two types of equation begin to diverge.

Since both the power type and exponential type of function appear to be equally capable of providing a satisfactory mathematical equation for a curved Mohr envelope over the range of stabilities to be considered in bituminous pavement design, the selection of one or the other type of function for this purpose may be a matter of personal preference. In this paper, the power function type that provides a parabolic equation has been chosen.

The various steps in the mathematical treatment involved when the parabolic equation is employed in this manner are listed in the

appendix. Values for L , V , s , n , c , and ϕ in the form of relatively simple equations derived from the use of this parabolic equation are also given in the appendix, for any Mohr circle.

Step No. 5 - Mathematical Solution for c and ϕ Values

By means of the detailed mathematical treatment given to this problem in the appendix, the following equations are derived for c and ϕ :

$$\phi = \tan^{-1} mr (n, - b)^{r-1} \quad (23)$$

$$c = s_c - n_c \tan \phi \quad (24)$$

where

m , b , and r = constants in the parabolic equation, Figures 26 and 27, and

n_c and s_c = the normal stress and shear stress, respectively, at the point of tangency between the curved Mohr envelope and the Mohr circle representing the conditions of stress in the prism of pavement just below the contact area. This point of tangency is at I in Figure 26, where the lateral support is considered to be equal to the unconfined compressive strength of the paving mixture U , and at F in Figure 27, where the lateral support is considered to be equal to the unconfined compressive strength U multiplied by a factor K .

For the stress conditions represented by Mohr circle (2) in Figure 26, this rigorous mathematical approach indicates the following values for c and ϕ :

$$c = 16.4 \text{ psi.}$$

$$\phi = 17^\circ 57'$$

while for the stress conditions represented by Mohr circle (3) in Figure 27, the values for c and ϕ are:

$$c = 17.5 \text{ psi.}$$

$$\phi = 17^\circ 05'$$

In each case, these are the values of c and ϕ required for substitution in equations (18), (19), (20), and (21), for determining the stability V of a bituminous paving mixture with the curved Mohr envelope illustrated in Figures 26 and 27.

COMPARISON OF STABILITY VALUES, CURVED VERSUS
STRAIGHT MOHR ENVELOPES

From the previous section of this paper, and from the appendix, it is apparent that determining the stability of a paving mixture with a curved Mohr envelope involves some time and trouble, particularly if the method of rigorous mathematical calculation is employed. The question arises of whether the margin of error resulting when a straight line Mohr envelope is assumed to represent the triaxial data, instead of the curved Mohr envelope that actually represents these data, justifies the greater effort that must be made when the stability determination is based on a curved Mohr envelope.

In the principal stress diagram of Figure 25(a), the curved line relationship between the V and L values is quite evident, although the degree of curvature is not pronounced. This principal stress diagram is reproduced in Figure 29(a), together with the best curved line through the points, but in addition, the best straight line established by the method of least squares is drawn through the data. Corresponding V and L values from the best straight line through the points of Figure 29(a) provide the straight line Mohr envelope of Figure 29(b), while V and L values from the best curved line in Figure 29(a) give the curved Mohr envelope of Figure 29(b).

Assuming in each case that the lateral support provided by the portion of the pavement just outside of the contact area is equal to the unconfined compressive strength, two Mohr circles (solid line) are drawn tangent to the curved Mohr envelope as shown, and two other Mohr circles (dashed line) are drawn tangent to the straight Mohr envelope. On the basis of the previous subject matter of this paper, if the frictional resistance between pavement and tire and between pavement and base were both equal to zero, Figure 29(b) shows that $V_c = 109.2$ psi. is the ultimate strength of the pavement if it is represented by the curved Mohr envelope, while $V_c = 118$ psi. is the ultimate strength of the pavement if it is represented by the straight line Mohr envelope. Under these conditions, the assumption of a straight line Mohr envelope would lead to a stability evaluation about 8 per cent too high.

From either Figure 26, or the example of calculations given in the appendix, the values for c and ϕ for the tangent to the curved envelope at its point of tangency I with the second Mohr circle from the left (solid line) in Figure 29(b) are $c = 16.4$ psi. and $\phi = 17^\circ 57'$, while for the straight line Mohr envelope in Figure 29(b) they are $c = 13.4$ psi. and $\phi = 20^\circ 20'$; that is, as would be

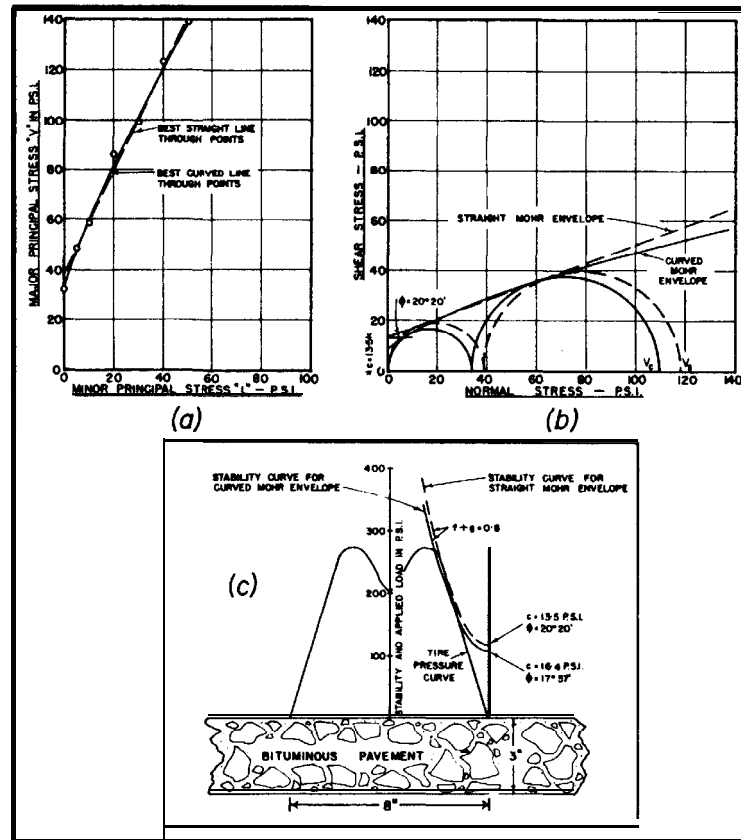


Fig. 29. Comparison of Stability Values Given by the Best Curved Line Through V and L Values Plotted on a Principal Stress Diagram (Resulting in a Curved Mohr Envelope) Versus Those Provided by the Best Straight Line Through the Same Points (Resulting in a Straight Mohr Envelope).

expected, the c and ϕ values provided by the straight line and curved line Mohr envelopes of Figure 29(b) are materially different.

On the basis of these c and ϕ values, the tire pressure distribution curve shown in Figure 29(c), and letting $f + g = 0.8$ in each case, stability curves can be drawn, Figure 29(c), assuming in one case that the stability of the paving mixture is represented by a straight Mohr envelope, and in the other case by a curved Mohr envelope. In the case of the straight Mohr envelope, equations (11) or (17) can be employed for determining the location of the corresponding stability curve, while for the curved Mohr envelope, the location of the required stability curve is given by equations (19) or (21). The stability curve for the straight line Mohr envelope becomes tangent to the tire pressure curve at a point two

inches from the edge of the contact area, and at a pressure or stability value of about 262 psi. At this same distance from the edge of the contact area, the stability value given by the stability curve for the curved Mohr envelope is about 242 psi.; that is, the stability of the latter is about 20 psi. less than the pressure applied by the tire at this point. Therefore, the difference between these two stability values is also about 8 percent. Consequently, on the basis of the paving mixture represented by Figure 29, assuming a straight line Mohr envelope located by the method of least squares, for a bituminous mixture for which the Mohr envelope is actually curve, could result in underdesign to the extent of about 8 percent.

From Figures 23(c), 24(c), 26, 27, and 28, it will be observed that the sharpest curvature of a curved Mohr envelope occurs at the left hand side of the Mohr diagram, and that the degree of curvature becomes progressively less as the envelope is extended to the right. The curvature of the best smooth curve in the principal stress diagram of Figure 29(a), and of the curved Mohr envelope in Figure 29(b) is not large, and a considerable difference in stability values obtained by treating the triaxial data on the basis of either a straight or curved Mohr envelope might not, therefore, be expected. Consequently, other examples in which much more curvature has been introduced into the smooth curve in the principal stress diagram, and into the corresponding curved Mohr envelope, have been investigated in a similar manner. Nevertheless, if the straight line Mohr envelope is located by the method of least squares, the maximum difference in stability that has been found by assuming a straight Mohr envelope for a bituminous mixture for which the Mohr envelope is actually curved, is less than 20 percent, the stability value for the straight Mohr envelope always being the larger. For the design of bituminous mixtures with curved Mohr envelopes, therefore, the assumption of a straight Mohr envelope located by the method of least squares will lead to stability underdesign to an extent that should not exceed about 20 percent as a maximum value, and may ordinarily be not more than about 10 percent.

DISCUSSION

1. In the section of this paper dealing with the design of bituminous paving mixtures with curved Mohr envelopes, the assumption is made that the critical **Mohr** circle is the one for which the entire lateral support L is provided by the portion of the pavement immediately adjacent to the loaded area, and is equal to either the unconfined compressive strength U of the paving mixture,

Mohr circle (2) in Figure 26, or to U multiplied by a factor K , Mohr circle (3) in Figure 27. It is believed that this assumption should lead to values for c and ϕ , provided by the tangent to the Mohr envelope at its point of tangency with the critical Mohr circle, that enable the stability curve, Figure 29(c), to be drawn with sufficient accuracy for purposes of pavement design.

Nevertheless, it should be observed that a critical Mohr circle, for which the lateral support L_S is provided by the pavement immediately adjacent to the loaded area, represents the stability of an element of pavement only at the edge of the contact area. For elements within the pavement at points between the edge and the centre of the contact area, the total lateral support $L = L_S + L_R$, where L_S is the lateral support provided by the pavement just outside the loaded area, and L_R is the equivalent lateral support due to the frictional resistances between pavement and tire and between pavement and base acting over the distance between the edge of the contact area and the position of the element under the contact area. To the extent that permissible strain within the pavement permits the equivalent lateral support L_R to be developed under traffic, it can provide an additional source of lateral support. The effect of the development of equivalent lateral support L_R would be to displace the position of the critical Mohr circles (2) and (3) in Figures 26 and 27 farther to the right. The length of the shift to the right through which the critical Mohr circle would be moved in either case would be governed by the distance from the edge of the contact area to the point where the stability curve is just tangent to the tire pressure curve, Figures 2, 13, 14, 29(c), etc. For the conditions illustrated by Figure 29(c), at this point of tangency the developed stability V required is about 250 psi. On this basis, the critical Mohr circle in Figures 26 and 27 would be moved to the right until the value of V , the major principal stress, was about 250 psi. From Figures 26 and 27, it is apparent that at the point of tangency of such a critical Mohr circle with the curved Mohr envelope, the angle of internal friction ϕ given by the tangent would be somewhat less, and cohesion c would be somewhat of an element of pavement only at the edge of the contact area. For elements within the pavement at points between the edge and the centre of the contact area, the total lateral support $L = L_S + L_R$, where L_S is the lateral support provided by the pavement just outside the loaded area, and L_R is the equivalent lateral support due to the frictional resistances between pavement and tire and between pavement and base acting over the distance between the edge of

the contact area and the position of the element under the contact area. To the extent that permissible strain within the pavement permits the equivalent lateral support L_R to be developed under traffic, it can provide an additional source of lateral support. The effect of the development of equivalent lateral support L_R would be to displace the position of the critical Mohr circles (2) and (3) in Figures 26 and 27 farther to the right. The length of the shift to the right through which the critical Mohr circle would be moved in either case would be governed by the distance from the edge of the contact area to the point where the stability curve is just tangent to the tire pressure curve, Figures 2, 13, 14, 29(c), etc. For the conditions illustrated by Figure 29(c), at this point of tangency the developed stability V required is about 250 psi. On this basis, the critical Mohr circle in Figures 26 and 27 would be moved to the right until the value of V , the major principal stress, was about 250 psi. From Figures 26 and 27, it is apparent that at the point of tangency of such a critical Mohr circle with the curved Mohr envelope, the angle of internal friction ϕ given by the tangent would be somewhat less, and cohesion c would be somewhat larger, than for Mohr circles (2) and (3). On the other hand, the change in curvature of the curved Mohr envelope over this additional distance is relatively small, and the change in c and ϕ , therefore, is likely to be small enough that it might not, even in an extreme case of a Mohr envelope of considerable curvature, shift the position of the stability curve, Figure 29(c), sufficiently to have any practical effect on the design requirements.

It might be added that not enough is yet known about the magnitudes of either L_S or L_R that can be mobilized within a pavement to support an applied load without developing sufficient strain to damage the pavement. For this reason, Figures 26, 27, 28, and 29 would appear to be not unsuitable for illustrating the principles of design that bituminous mixtures with curved Mohr envelopes involve. This is particularly true of Figure 27, since in a broad sense, Mohr circle (3), for which the lateral support L is equal to the unconfined compressive strength U multiplied by a factor K , could be considered to include every item in the two variables L_S and L_R , and from other sources, if any, that contributes to the overall effective lateral support L for any element of pavement for which the stability under load is desired.

2. Expressing the **portion** of the curved Mohr envelope required for pavement design in the form of a **mathematical** equation,

and carrying through the calculations to provide the values for c and ϕ given by the tangent at the point of tangency between the critical Mohr circle and the curved Mohr envelope requires some time. It is believed that for ordinary pavement design, sufficient accuracy would be obtained by a graphical solution. This requires that the best smooth curve be drawn tangent to the Mohr circles, and that a tangent be drawn by visual inspection at the point of tangency between the curved Mohr envelope and the critical Mohr circle. The angle of internal friction ϕ and cohesion c given by this tangent can be readily measured.

Alternatively, as developed in the previous section, it seems not unlikely that a straight line Mohr envelope, located by the method of least squares on the Mohr diagram for a bituminous mixture with a curved Mohr envelope, may provide c and ϕ values that are close enough for practical pavement design. While this method seems to always lead to some underdesign, it appears that the degree of underdesign would not exceed 20 percent in an extreme case, and might not ordinarily exceed 10 percent in the great majority of cases.

3. While the subject matter of this paper has been presented quantitatively, it is clearly realized that other theoretical equations could be employed or developed that would provide somewhat different quantitative values than those that are shown in a number of diagrams. It should be emphasized in this connection, however, that the primary purpose of the paper has been to illustrate the principles by means of which stability problems presented by bituminous paving mixtures with curved Mohr envelopes might be solved, rather than to cover all the mathematical equations that might be employed to provide the quantitative answers required.
4. Finally, until there has been an opportunity to build up information on the field performance of bituminous mixtures designed by the rational method based upon the triaxial test, it would be prudent to employ a generous safety factor. In this connection, it should be emphasized that the values for stability V provided by any of the equations contained in the latter part of this paper represent the ultimate resistance of the pavement to being squeezed out between the tire and the base course. The strain that occurs within the pavement when this ultimate strength is developed may be large enough to cause permanent damage to the pavement. For this reason, a safety factor may have to be applied to the ultimate strength V provided by equations (10), (11), (16), (17), (18), (19), (20), or (21), in order to keep the

strain developed by the pavement, when under load, small enough to avoid permanent pavement injury. It must also be recognized that until the required experimental work can be undertaken in both the laboratory and the field, not enough is known about the actual shape of the tire pressure distribution curve across the contact area for different tires, or about the magnitude of such variables as K , f , g , P , Q , n , t , etc., to make adequate use of them for the design of bituminous pavements at the present time. It is for these reasons that a generous safety factor is suggested when the above equations provided by the rational method are employed.

Nevertheless, if particular care is taken to obtain a strong bond between pavement and base, if design is based upon the stationary load condition, and for the maximum pressure applied to the contact area, and if it is assumed that the factor $K = 1$, it is believed that equation (3) or the design curves of Figure 7 provide a conservative basis for design, which is illustrated by stability curve number (2) in Figure 2. It is believed that no safety factor is required in this case, since an ample factor of safety seems to be provided by the neglect of such variables as f , g , P , Q , n , t , etc., when design is based upon equation (3) or Figure 7. For bituminous mixtures with curved Mohr envelopes, the required values for c and ϕ to be employed with equation (3) or Figure 7 can apparently be obtained with sufficient accuracy from the best straight line Mohr envelope through the Mohr diagram, located by the method of least squares.

Since the use of equation (3) and Figure 7 provides an unknown safety factor that may be of considerable magnitude, it is believed that it would be very much worth while if such variables as K , f , g , P , Q , n , t , etc., could be evaluated experimentally as soon as possible. This would enable equations such as (10), (11), (16), (17), (18), (19), (20), and (21) and a controlled safety factor to be employed for bituminous pavement design.

SUMMARY

- (1) A rational approach to the design of bituminous paving mixtures with straight line Mohr envelopes described in an earlier paper is reviewed.
- (2) All present methods for the design of bituminous pavements indicate that to support the much higher tire pressures of jet aircraft, a bituminous pavement of greater stability must be provided.

- (3) As an alternative solution to this problem of pavement design for high tire pressures, the rational approach to bituminous pavement design suggests that bituminous pavements of relatively low stability might be stable under these higher average tire pressures, if a multiple-compartment tire were used with the highest inflation pressure in the innermost compartment, and the lowest pressure in the outermost compartment.
- (4) A rational approach to the design of bituminous paving mixtures with curved Mohr envelopes is described. Both a graphical solution for this purpose and a rigorous mathematical method are given.
- (5) It is shown that for bituminous mixtures with curved Mohr envelopes, straight line Mohr envelopes drawn through the Mohr diagram, and located by the method of least squares, provide stability values that may be from 10 to 20 percent too high, but may nevertheless be sufficiently accurate for practical pavement design at the present time.

ACKNOWLEDGEMENTS

The material presented in this paper forms part of an extensive investigation of airports in Canada that was begun by the Canadian Department of Transport in 1945. Air Vice-Marshal A. T. Cowley, Director of Air Services, has the general administration of this investigation. It comes under the direct administration of Mr. Harold J. Connolly, Superintendent Construction, Mr. George W. Smith, Assistant Superintendent Construction, and Mr. E. B. Wilkins. In their respective districts, the investigation is carried on with the generous cooperation of District Airway Engineers G. T. Chillcott, J. H. Curzon, F. L. Davis, O. G. Kelly, L. Millidge, and W. D. G. Stratton.

For their able assistance with the calculations on which this paper is based, and for their skillful drafting of the diagrams, the author wishes to make grateful acknowledgement to Mr. C. L. Perkins particularly, and to Mr. Edwin K. Parks and Mr. John Ruptash.

REFERENCES

1. Norman W. McLeod, "The Rational Design of Bituminous Paving Mixtures," Proceedings, Highway Research Board, Volume 29 (1949).
2. Norman W. McLeod, "A Rational Approach to the Design of Bituminous Paving Mixtures," Proceedings, The Association of Asphalt Paving Technologists, Volume 19 (1950).

3. Norman W. McLeod, "Application of Triaxial Testing to the Design of Bituminous Pavements, " American Society for Testing Materials Special Technical Publication 106 (1951) .
4. L. W. Teller and J. A. Buchanan, "Determination of Variation in Unit Pressure over the Contact Area of Tires, " Public Roads, Volume 18, No. 10 (1937).
5. O. J. Porter, "Accelerated Traffic Test at Stockton Airfield, Stockton, California, " (Stockton Test No. 2) Corps of Engineers, Sacramento District, March (1949) .
6. A. H. D. **Markwick** and H. J. H. Starks, "Stress Between Tire and Road," Journal, The Institution of Civil Engineers, Volume 16 (1940-41).
7. R. A. Moyer, "**Motor** Vehicle Operating Costs, Road Roughness, and Slipperiness of Various Bituminous and Portland Cement Concrete Surfaces, " Proceedings, Highway Research Board, Volume 22 (1942).
8. C . G. Giles and A. R. Lee, "Non-Skid Roads, " Proceedings, The Public Health and Municipal Engineering Congress, November (1948).
- 9 . Leo Jurgenson, "**The** Shearing Resistance of Soils, " Contributions to Soil Mechanics 1925-1940, Boston Society of Civil Engineers (1940) .
10. "Manual on Hot-Mix Asphaltic Concrete Paving, " **The Asphalt Institute**, New York, N.Y ., U.S.A. (1945).
11. Norman W. McLeod, "Tire Design, Pavement Design, and Vehicle Mobility, " Proceedings, Highway Research Board, Volume 31 (1952).
12. Glenn Murphy, "Advanced Mechanics of Materials, " **McGraw-Hill Book Co.**, Incorporated, New York, First Edition, p. 24 (1946).
13. R. G. Hennes and C. C. Wang, "Physical Interpretation of Triaxial Test Data," Proceedings, The Association of Asphalt Paving Technologists, Volume 20 (1951).
14. A. Casagrande and N. Carrillo, "Shear Failure of Anisotropic Materials," Journal, Boston Society of Civil Engineers, April (1944) .
15. R. J. Hank and L. E. McCarty, "**Shear** Failure in Anisotropic Materials Possessing any Values of Cohesion and Angle of Internal Friction, " Proceedings, Highway Research Board, Volume 28 (1948).
16. Dale S. Davis, "Empirical Equations and Nomography, " **McGraw-Hill Book Co., Inc .**, New York, First Edition (1943).

APPENDIX

ANALYSIS OF MOHR DIAGRAMS WITH CURVED
MOHR ENVELOPES

In the Mohr diagrams of Figures 26 and 27, let the curved Mohr envelope be represented by the parabolic equation

$$s = m (n - b)^r \quad (25)$$

where

m , b , and r are constants,
 n and s are normal stress and shear stress, respectively.

In Figures 26 and 27, the equation for Mohr circle (1) representing the unconfined compressive strength is

$$\left(n - \frac{U}{2} \right)^2 + s^2 = \left(\frac{U}{2} \right)^2$$

which, upon rearranging and simplifying, becomes

$$s^2 = nU - n^2 \quad (26)$$

where

U = unconfined compressive strength
 n and s = normal and shear stress, respectively, on any plane through the test specimen subjected to the unconfined compressive strength U .

In Figure 26, the equation for Mohr circle (2), for which the lateral support L_2 is equal to the unconfined compressive strength U , is

$$\left[n - \left(\frac{V_2 + U}{2} \right) \right]^2 + s^2 = \left(\frac{V_2 - U}{2} \right)^2$$

which, upon rearranging and simplifying, becomes

$$s^2 = n (V_2 + U) - n^2 - V_2 U \quad (27)$$

where

V_2 = the major principal stress when the lateral support L_2 is equal to the unconfined compressive strength U ,
 n and s = normal and shear stresses on any plane through the specimen when the principal stresses are V_2 and U .

In Figure 27, the equation for any Mohr circle (3), for which the principal stresses are V_3 and L_3 , where $L_3 = KU$, is

$$\left[n - \left(\frac{V_3 + L_3}{2} \right) \right]^2 + s^2 = \left(\frac{V_3 - L_3}{2} \right)^2$$

which, upon rearranging and simplifying, becomes

$$s^2 = n(V_3 + L_3) - n^2 - V_3 L_3 \quad (28)$$

where

V_3 and L_3 = major and minor principal stresses, and $L_3 = KU$,
 n and s = normal and shear stresses on any plane through
the specimen when the principal stresses are V_3
and L_3 .

In Figures 26 and 27, the slope of the tangent at any point on the curved Mohr envelope is given by the first derivative of equation (25),

$$\frac{ds}{dn} = mr (n - b)^{r-1} \quad (29)$$

In Figures 26 and 27, the slope of the tangent at any point on the circumference of Mohr circle (1) is given by the first derivative of equation (26)

$$\frac{ds}{dn} = \frac{U - 2n}{2s} \quad (30)$$

In Figure 26, the slope of the tangent at any point on the circumference of Mohr circle (2) is given by the first derivative of equation (27),

$$\frac{ds}{dn} = \frac{V_2 + U - 2n}{2s} \quad (31)$$

In Figure 27, the slope of the tangent at any point on the circumference of Mohr circle (3) is given by the first derivative of equation (28),

$$\frac{ds}{dn} = \frac{V_3 + L_3 - 2n}{2s} \quad (32)$$

Analysis of Mohr Circle (1) Representing Unconfined Compression, Figures 26 and 27

For Mohr circle (1) in Figures 26 and 27, values are required for U , the unconfined compressive strength, for n_u and s_u , the normal and shear stress coordinates for the point of tangency G between the curved Mohr envelope and Mohr circle (1), and for c_u and ϕ_u given by the tangent to the curved Mohr envelope at G .

At the point of tangency, G, between the curved Mohr envelope and Mohr circle (1), the equation for the curved Mohr envelope is

$$s_u = m (n_u - b)^r \quad (25a)$$

and the equation for Mohr circle (1) is

$$s_u^2 = n_u U - n_u^2 \quad (26a)$$

Squaring equation (25a), equating it to equation (26a), and rearranging, gives

$$U = \frac{m^2 (n_u - b)^{2r} + n_u^2}{n_u} \quad (33)$$

At the point of tangency, G, the slopes of the tangents to Mohr circle (1) and to the curved Mohr envelope are equal; that is, equating equations (29) and (30), and introducing appropriate subscripts, gives

$$mr (n_u - b)^{r-1} = \frac{u - 2n_u}{2s_u}$$

which, upon substituting the right hand side of equation (25a) for s_u , simplifying, and rearranging, becomes

$$U = 2m^2 r (n_u - b)^{2r-1} + n_u^2 \quad (34)$$

Equating equations (33) and (34), and simplifying, gives

$$m^2 (n_u - b)^{2r} - 2m^2 n_u r (n_u - b)^{2r-1} - n_u^2 = 0 \quad (35)$$

In equation (35), m , b , and r are the constants in equation (25), which represents the curved Mohr envelope, and values for them are given in Figures 26 and 27. The method for evaluating each of the three constants m , b , and r is illustrated in the example of calculations given at the end of this section of the appendix. Therefore, the value for n_u required to satisfy equation (35) can be quickly determined from a graphical plot of equation (35) versus trial values for n_u , Figure 30(b).

By substituting the value for n_u found in this manner in equations (33) or (34), the value for U can be calculated, since the values for m , b , and r have been established.

In addition, since the values for n_u , m , b , and r have been ascertained, values for s_u , ϕ_u , and c_u can be calculated from the following equations

$$s_u = m (n_u - b)^r \quad (25a)$$

$$\phi_u = \tan^{-1} mr (n_u - b)^{r-1} \quad (36)$$

$$c_u = s_u - n_u \tan \phi_u \quad (37)$$

Because it would add to the detail of the diagrams, the tangent to Mohr circle (1) at its point of tangency with the curved Mohr envelope is not shown in either Figure 26 or 27.

Analysis of Mohr Circle (2), Figure 26

For Mohr circle (2) in Figure 26, for which the lateral pressure L_2 is equal to the unconfined compressive strength U , values are required for V_2 , the major principal stress, for n_2 and s_2 , the normal and shear stress coordinates for the point of tangency, I, between the curved Mohr envelope and Mohr circle (2), and for c_2 and ϕ_2 given by the tangent to the curved Mohr envelope at I.

At the point of tangency, I, the equations for the curved Mohr envelope and for Mohr circle (2) are

$$s_2 = m (n_2 - b)^r \quad (25b)$$

and

$$s_2^2 = n_2 (V_2 + u) - n_2^2 - V_2 U \quad (26b)$$

Squaring equation (25b), equating it to equation (26b), and rearranging, gives

$$V_2 = \frac{m^2 (n_2 - b)^{2r}}{n_2 - U} + n_2 \quad (38)$$

At the point of tangency, I, the slopes of the tangents to the curved envelope and Mohr circle (2) are equal. Therefore, equating equations (29) and (31), introducing the appropriate subscripts, and rearranging, (remembering that $s_2 = m (n_2 - b)^r$), gives

$$V_2 = 2m^2 r (n_2 - b)^{2r-1} - U + 2n_2 \quad (39)$$

Equating equations (38) and (39), and simplifying, gives

$$m^2 (n_2 - b)^{2r} - 2m^2 r (n_2 - b)^{2r-1} (n_2 - U) + 2n_2 U - U^2 - n_2^2 = 0 \quad (40).$$

In equation (40), values for the constants m , b , and r from equation (25) for the curved Mohr envelope are given in Figures 26 and 27 (see the example of calculations at end of this appendix for a method for their evaluation), the value for U has already been determined for Mohr circle (1), and n_2 is, therefore, the only unknown. The value for n_2 required to satisfy equation (40) can be quickly determined from a graphical plot equation (40) versus trial values for n_2 , Figure 30(c).

By substituting the value for n_2 found by this means in equations (38) or (39), the value of V_2 can be calculated, since the values for m , b , r , U , and n_2 have been established.

In addition, since the values for n_2 , m , b , and r have been ascertained, values for s_2 , θ_2 , and c_2 can be calculated from the following equations.

$$s_2 = m (n_2 - b)^r \quad (25b)$$

$$\theta_2 = \tan^{-1} m r (n_2 - b)^{r-1} \quad (41)$$

$$c_2 = s_2 - n_2 \tan \theta_2 \quad (42)$$

Analysis of Mohr Circle (3), Figure 27

For any Mohr circle (3), Figure 27, for which the lateral pressure L_3 is equal to KU , where KU is the unconfined compressive strength U multiplied by a specified factor K , values are required for V_3 , the major principal stress, for n_3 and s_3 , the normal and shear stress coordinates for the point of tangency, F , between the curved Mohr envelope and Mohr circle (3), and for c_3 and θ_3 given by the tangent to the curved Mohr envelope at F .

At the point of tangency, F , the equations for the curved Mohr envelope and for Mohr circle (3) are

$$s_3 = m (n_3 - b)^r \quad (25c)$$

and

$$s_3^2 = n_3 (V_3 - L_3) - n_3^2 - V_3 L_3 \quad (26c)$$

Squaring equation (25c), equating it to equation (26c), and rearranging, gives

$$V_3 = \frac{m^2 (n_3 - b)^{2r}}{n_3 - L_3} + n_3 \quad (43)$$

At the point of tangency, F , the slopes of the tangents to the curved envelope and Mohr circle (3) are equal. Therefore, equating equations (29) and (32), introducing the appropriate subscripts, and rearranging (remembering that $s_3 = m (n_3 - b)^r$), gives

$$V_3 = 2m^2 r (n_3 - b)^{2r-1} - L_3 + 2n_3 \quad (44)$$

Equating equations (43) and (44), and simplifying, gives

$$m^2 (n_3 - b)^{2r} - 2m^2 r (n_3 - b)^{2r-1} (n_3 - L_3) + 2n_3 L_3 - L_3^2 - n_3^2 = 0 \quad (45)$$

In equation (45), values for the constants m , b , and r , from equation (25) for the curved Mohr envelope, are given in Figures 26 and 27 (see example of calculations at the end of this appendix for a method for their evaluation), the value of $L_3 = KU$ is known, since the value of K to be used is specified, and the value of U has already been determined for Mohr circle (1), and n_3 is, therefore,

the only unknown. The value for n_3 required to satisfy equation (45) can be quickly determined from a graphical plot of equation (45) versus trial values for n_3 , similar to Figure 30(c).

By substituting the value for n_3 found by this means in equations (43) or (44), the value for V_3 can be calculated, since the values for m , b , r , L_3 , and n_3 have been established. It will be remembered that $L_3 = KU$, where the value of K is specified, and the value of U , the unconfined compressive strength, has already been determined for Mohr circle (1).

In addition, since the values for n_3 , m , b , and r have been ascertained, values for s , ϕ_3 , and c_3 can be calculated from the following equations.

$$s_3 = m (n_3 - b)^r \quad (25c)$$

$$\phi_3 = \tan^{-1} mr (n_3 - b)^{r-1} \quad (46)$$

$$c_3 = s_3 - n_3 \tan \phi_3 \quad (47)$$

AN EXAMPLE OF CALCULATIONS

To Evaluate the Constants m , b , and r in the Parabolic Equation Representing the Curved Mohr Envelope

It will be assumed that points representing the V and L values provided by a triaxial test on a bituminous paving mixture with a curved Mohr envelope have been plotted on a principal stress diagram, and that the best smooth curve has been drawn through them, e.g., Figure 25(a). Using V and L values from well-distributed points on this curve, describe a number of Mohr circles, e.g., Figures 23(c), 24(c), 26, and 27, and draw a smooth curve tangent to the Mohr circles. Select three points, X , Y , and Z , on this curved Mohr envelope, Figure 26, of such spacing that point X is slightly to the right of the point of tangency, G , of the curved Mohr envelope with Mohr circle (1) representing the unconfined compressive strength, point Z is somewhat to the right of tie point of tangency of the curved envelope with the Mohr circle considered to represent the stability of the pavement; that is, somewhat to the right of I in Figure 26, and of F in Figure 27; while point Y is approximately half-way between them.

As precisely as they can be read from the curved Mohr envelope of Figure 26, the normal stress and shear stress (n and s) coordinates for points X , Y , and Z are as follows:

	$\frac{n}{\text{lb}}$	$\frac{s}{\text{lb}}$
X	10	15.5
Y	40	28.9
Z	80	42.0

The parabolic equation assumed to represent the curved Mohr envelope over the range of stress under consideration is:

$$s = m (n - b)^r \quad (25)$$

Equation (25) contains three constants, m , b , and r , and the two variables normal stress n and shear stress s . The three constants m , b , and r can be evaluated by substituting the n and s values for the three points X, Y, and Z in equation (25) to form three equations that can be solved simultaneously. These three equations are:

$$15.5 = m (10 - b)^r \quad (a)$$

$$28.9 = m (40 - b)^r \quad (b)$$

$$42.0 = m (80 - b)^r \quad (c)$$

Combining equations (a) and (b), and equations (b) and (c), gives

$$15.5 (40 - b)^r = 28.9 (10 - b)^r \quad (d)$$

and

$$28.9 (80 - b)^r = 42.0 (40 - b)^r \quad (e)$$

Substitute trial values for b in equation (d) and calculate corresponding values for r . Substitute the values for b and r so obtained in equation (e), and plot the left hand side of equation (e) minus the right hand side against the trial values for b , Figure 30(a). When this difference is zero, the correct value for b has been obtained. Figure 30(a) indicates that the correct value for $b = -6.5$

When the correct value for b , -6.5 , is substituted in equation (d), it is found that $r = 0.6$. These values for b and r are also found to satisfy equation (e), which serves as a check.

When the values $b = -6.5$ and $r = 0.6$ are substituted in equations (a), (b), and (c), it is found that the value for $m = 2.89$.

Therefore, the required values for the constants m , b , and r in equation (25) are

$$m = 2.89$$

$$b = -6.5$$

$$r = 0.6$$

Analysis of Mohr Circle (1), Unconfined Compression, Figures 26 and 27

The value for n_u at the point of tangency, G, between the curved Mohr envelope and Mohr circle (1), Figure 26, where n_u represents

the normal stress on the plane of failure for the unconfined compressive strength condition, can be calculated from equation (35),

$$m^2 (n_u - b)^{2r} - 2m^2 n_u r (n_u - b)^{2r-1} - n_u^2 = 0 \tag{35}$$

Values for the constants m , b , and r have already been determined, and the value of n_u can be found graphically by plotting equation (35) against trial values for n_u until this equation is satisfied. Figure 30(b) illustrates this method, and indicates that the required value for $n_u = 8.32$ psi.

By substituting the values determined for m , b , r , and n_u in equations (33) or (34), the value of U , the unconfined compressive strength, Figure 26 and 27, can be calculated.

$$U = \frac{m^2 (n_u - b)^{2r} + n_u^2}{n_u} \tag{33}$$

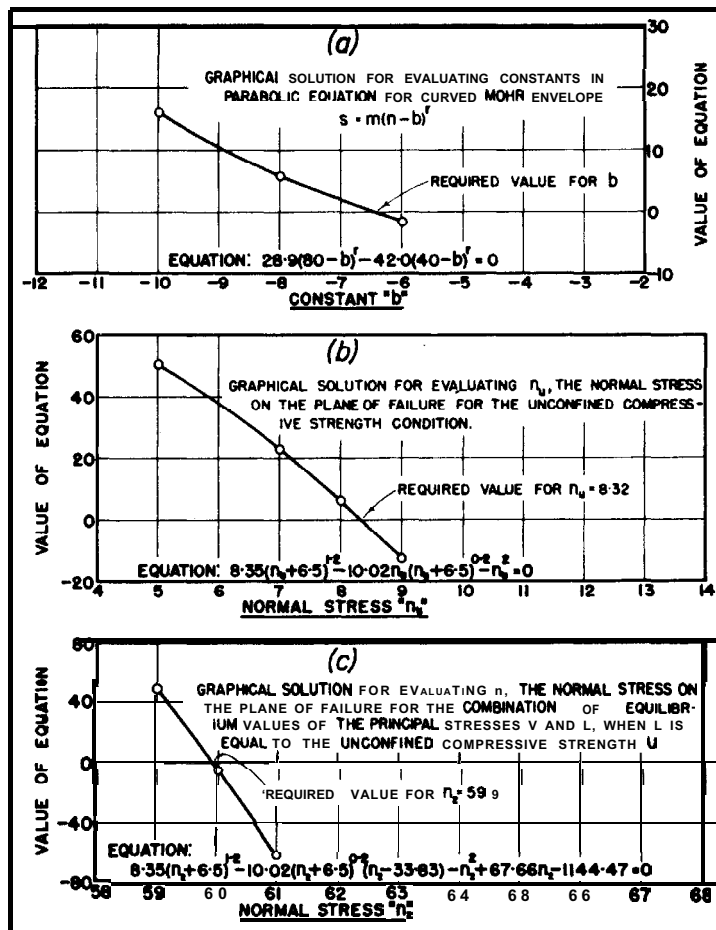


Fig. 30. Illustrating Graphical Methods for Simplifying the Solution of Three Key Equations Associated with Curved Mohr Envelopes.

from which

$$U = 33.83 \text{ psi.}$$

From the values for m , b , r , and n_u that have been established, values for s_u , ϕ_u , and c_u can be easily calculated by means of equations (25a), (36), and (37).

$$\text{from which} \quad s_u = m (n_u - b)^r \quad (25a)$$

$$s_u = 14.6 \text{ psi.}$$

$$\text{from which} \quad \phi_u = \tan^{-1} mr (n_u - b)^{r-1} \quad (36)$$

$$\phi_u = 30^\circ 32'$$

$$\text{from which} \quad c_u = s_u - n_u \tan \phi_u \quad (37)$$

$$c_u = 9.7 \text{ psi.}$$

Consequently, for Mohr circle (1) in Figures 26 and 27,

$$U = 33.8 \text{ psi.}$$

$$n_u = 8.3 \text{ psi.}$$

$$s_u = 14.6 \text{ psi.}$$

$$c_u = 9.7 \text{ psi.}$$

$$\phi_u = 30^\circ 32'$$

Analysis of Mohr Circle (2), Figure 26

The value for n_2 at the point of tangency I between the curved Mohr envelope and Mohr circle (2), Figure 26, where n_2 represents the normal stress on the plane of failure when the principal stresses are V_2 and $L_2 = U$, can be calculated from equation (40).

$$m^2 (n_2 - b)^{2r} - 2m^2 r (n_2 - b)^{2r-1} (n_2 - U) + 2n_2 U - U^2 - n_2^2 = 0 \quad (40)$$

Values for the constants m , b , and r , and for the unconfined compressive strength U have already been determined, and the value for n_2 can be found graphically by plotting equation (40) against trial values for n_2 until this equation is satisfied. Figure 30(c) illustrates this method and indicates that the required value for $n_2 = 59.9 \text{ psi.}$

By substituting the values determined for m , b , r , U , and n_2 in equations (38) or (39), the value of V_2 , the major principal stress, Figure 26, can be calculated.

$$V_2 = 2m^2r (n_2 - b)^{2r-1} - U + 2n_2 \quad (39)$$

from which

$$V_2 = 109.2 \text{ psi.}$$

From the values for m , b , r , and n_2 that have been established, values for s_2 , ϕ_2 , and c_2 can be easily calculated by means of equations (25b), (41), and (42).

$$s_2 = m (n_2 - b)^r \quad (25b)$$

from which

$$s_2 = 35.8 \text{ psi.}$$

$$\phi_2 = \tan^{-1} mr (n_2 - b)^{r-1} \quad (41)$$

from which

$$\phi_2 = 17^{\circ}57'$$

$$c_2 = s_2 - n_2 \tan \phi_2 \quad (42)$$

from which

$$c_2 = 66.4 \text{ psi.}$$

Consequently, for Mohr circle (2) in Figure 26,

$$U = 33.8 \text{ psi.}$$

$$V_2 = 109.2 \text{ psi.}$$

$$n_2 = 59.9 \text{ psi.}$$

$$s_2 = 35.8 \text{ psi.}$$

$$c_2 = 16.4 \text{ psi.}$$

$$\phi_2 = 17^{\circ}57'$$

Analysis of Mohr Circle (3), Figure 27, General Case

The value for n_3 at the point of tangency F between the curved Mohr envelope and Mohr circle (3), Figure 27, where n_3 represents the normal stress on the plane of failure when the principal stresses are V_3 and $L_3 = KU$, where $K = 1.2$ as an arbitrarily specified value in this example, and U is the unconfined compressive strength, can be calculated from equation (45).

$$m^2 (n_3 - b)^{2r} - 2m^2r (n_3 - b)^{2r-1} (n_3 - L_3) + 2n_3 L_3 - L_3^2 - n_3^2 = 0 \quad (45)$$

Values for the constants m , b , and r have already been determined, $L_3 = KU$, both K and U being known, and the value for n_3 can be found graphically by plotting equation (45) against trial values for n_3 until this equation is satisfied. The method is illustrated in Figure 30(c), which was employed to evaluate n_2 , and a

similar graph indicates that the required value for $n_3 = 69.1$ psi.

By substituting the values determined for m , b , r , and n_3 in equations (43) or (44), and remembering that $L_3 = KU$, the value of V_3 , the major principal stress, Figure 27, can be calculated.

$$V_3 = 2m^2r (n_3 - b)^{2r-1} - L_3 + 2n_3 \quad (44)$$

from which

$$V_3 = 121.4 \text{ psi.}$$

From the values for m , b , r , and n_3 that have been established, values for s_3 , ϕ_3 , and c_3 can be easily calculated by means of equations (25c), (46), and (47).

$$s_3 = m (n_3 - b)^r \quad (25c)$$

from which

$$s_3 = 38.7 \text{ psi.}$$

$$\phi_3 = \tan^{-1} mr (n_3 - b)^{r-1} \quad (46)$$

from which

$$\phi_3 = 17^\circ 5'$$

$$c_3 = s_3 - n_3 \tan \phi_3 \quad (47)$$

from which

$$c_3 = 17.5 \text{ psi.}$$

Consequently, for Mohr circle (3) in Figure 27,

$$L_3 = KU = (1.2) (33.8) = 40.6 \text{ psi.}$$

$$V_3 = 121.4 \text{ psi.}$$

$$n_3 = 69.1 \text{ psi;}$$

$$s_3 = 38.7 \text{ psi.}$$

$$c_3 = 17.5 \text{ psi.}$$

$$\phi_3 = 17^\circ 5'$$

Discussion

PROF. B. A. VALLERGA: Dr. McLeod, how did you arrive at the shape of your curved envelope?

MR. McLEOD: The shape of the curved Mohr envelope would result from plotting the triaxial data from certain bituminous paving mixtures.

PROF. VALLERGA: That is all right; by tests. The second question then is to what do you attribute the curvature?

MR. McLEOD: We have not been too much concerned with the cause of the curved Mohr envelope. We have assumed that a curved Mohr envelope is a fundamental characteristic of certain bituminous paving mixtures, and not an accidental effect due to improper dimensions of the test specimens, etc.

PROF. VALLERGA: I think we should be concerned. I think we should know why the envelope curves like that because, among other things, it would lead to a third question that I have. It has been suggested that the curvature is due to structural effects like interlocking and things of that sort. If that were the case, would that not lead you to suspect that the limiting curve would be a straight line through the origin? Do you understand what I am trying to say?

MR. McLEOD: There is one point I would like to make in connection with this discussion. Professor Vallerga has mentioned structural effects. The ratio of height to diameter of the test specimen could be taken as one of these. This paper has been based upon the assumption that dimensional and all other accidental or fortuitous effects are eliminated as a cause of the curvature of the Mohr envelope. It has been assumed, for example, that the test specimens are tall enough that the normal plane of failure will not intersect either end of the specimen. This would rule out test specimens of low height to diameter ratio, such as those employed for Marshall or Hveem Stabilometer tests, for which curved Mohr envelopes seem to result.

PROF. VALLERGA: In our triaxial work at the University of California, we use specimens of a height-diameter ratio such that the inhibiting effects of the upper and lower loaded boundaries of the sample are minimized. However, still we find for a crushed material or rock with large sized particles that we are not able to develop a straight line Mohr envelope that will go through the origin, and that we always have an intercept on the ordinate. Also we suspect that the envelope should be curved for reasons I will not go into here. Therefore, I have no particular argument with the curvature of your envelopes, because I think it can be explained by the relative size of the particles compared to the size of the container. It is because of this that a limiting curve for materials of successively smaller grain sizes would be a straight line through the origin.

MR. McLEOD: In view of the considerable published data for triaxial tests on bituminous paving mixtures, I find it difficult to believe that the Mohr envelopes for properly designed bituminous

mixtures would fail to show an intercept on the ordinate axis. Existing data do not verify the suggestion that Mohr envelopes for these mixtures pass through the origin. They invariably show a positive value for cohesion c .

PROF. VALLERGA: Let's eliminate the asphalt and talk about aggregates .

MR. McLEOD: This paper is concerned with the rational design of bituminous paving mixtures and we should probably stay with that subject.

PROF. VALLERGA: Then let us load a bituminous mix such that the viscosity and cohesion effects of the asphalt are zero. This bituminous mixture with zero viscosity effects would then behave like the aggregate without asphalt added.

MR. McLEOD: I very much doubt that any properly designed dense-graded bituminous paving mixture can be tested triaxially in such manner that its cohesion c becomes zero; or more precisely, that its cohesion becomes zero when the normal stress on the plane of failure is zero. It is a matter of common observation that the stability of moist sand on any sandy beach is superior to that of the same sand when dry due merely to the binding effect of the cohesion provided by the moisture films around the sand grains, and it is my understanding that when moist (not saturated) sands are tested triaxially, their Mohr envelopes show an intercept on the ordinate axis that we call cohesion c .

PROF. VALLERGA: I disagree. All our work at the University shows that for fine-grained sands tested triaxially at very low pressures, the Mohr envelope passes through the origin, provided effective pressures are plotted. For work carefully done, we can get the envelope through the origin in all cases, except where the particle size becomes great compared to the specimen size, i.e., where the structural effects would be all important. A large particle strategically located at the failure surface would materially affect the shearing resistance of the mass. If, on the other hand, these particles are small, the effects of structure become less apparent. For aggregates with relatively large size particles, the only possibility of minimizing this size effect would be to increase the size of the specimen.

MR. McLEOD: I believe it is generally agreed that no useful information can be obtained from testing bituminous paving mixtures by the triaxial method, unless the dimensions of the test specimen are large in comparison with the diameter of the largest

aggregate particles in the mixture. We cannot expect to obtain representative **stability** values if the test specimens are so small that one or more large particles on the plane of failure interfere materially with the results. There are two quite definite requirements for the test specimens of bituminous paving mixtures for triaxial tests. First, the test specimen must be tall enough with respect to its diameter that the stability value is not influenced by the constraints to which the ends of the specimen are unavoidably subjected **during** the test, and secondly, the dimensions of the test specimen must be large enough in comparison with the dimensions of the largest particles in the paving mixtures, that the stability value is not materially affected either by the fortuitous presence of a few more large particles on the plane of failure than their average distribution through the test specimen would permit, or by the fortuitous absence of the same number of larger particles from the plane of failure.

PROF. VALLERGA: What was the size of the specimen you used and what was the maximum size of the particle you used?

MR. McLEOD: This paper has presented a theoretical analysis of the design problem. However, those who have done considerable work on the triaxial testing of bituminous mixtures recommend that the diameter of the test specimen should be from four to six times the maximum dimension of the **largest particle**. The figure of four times may be a liberal value, while six times appears to be conservative.

PROF. VALLERGA: In order to what?

MR. McLEOD: In order to eliminate any material effect on the stability value due to either the presence of a few more large particles on the plane of failure than their average distribution through the test specimen would permit, or the absence of the same number of large particles on the plane of failure.

MR. V. A. ENDERSBY: What I am going to try to do is add a little more confusion to this argument. I just wanted to point out that it is a difficult job to **settle** this question. Let's see how the Mohr envelope is normally arrived at.

You draw the circles and then you draw a line tangent to them, and the closest you can get to the origin is where this line **comes** tangent with your zero circle. You don't know where it goes from there.- It can go straight on or come down through the origin on a curve, As a result of a lot of work done on that matter by Shell Development Company, we found that where you have a

curved envelope and this condition, your envelope acts like that, and if you adjust temperatures, pressures and speed of loading, you can get down to an extremely small zero circle here; the envelope comes tangent to that circle as it goes through the same origin, so unless you have a straight line through all of these circles, tangent to all of these circles, you will have no certainty that this projection actually represents something real. Even if you have a straight line tangent to all of them, it is only an inference that it continues straight all the way to the origin.

We found, though, that what has been said about interference of particles and dimensions and so on is quite correct. You get a very systematic family of curves as you shorten up the test specimen which implies pretty clearly that the reason for the curvature is an outside influence, and that ties in perfectly with what we are pointing out in particle arrangements. It has been obvious that the shorter your sample is, the more effect those particle arrangements are going to have. Therefore, my view of it is that this curvature represents such structural effect, pure and simple, and the extent of it depends on the dimensions of your sample. So I don't have any particular argument with either of the previous speakers, except that I wanted to show that it is not too sure what you have in the way of an intercept.

MR. N. W. McLEOD: If I understand Mr. Endersby's comments correctly, they imply that the curvature of the Mohr envelope when it occurs, is due to a low ratio of height to diameter for the test specimen, provided the ratio of specimen diameter to largest particle diameter is adequate. If curvature of the Mohr envelope could always be explained on this simple basis, it would greatly simplify bituminous pavement design. However, I am not too optimistic in that regard. As a matter of fact, it was assumed in the paper that curvature of the Mohr envelope is a fundamental property of certain bituminous mixtures, and curvature of the envelope due to what might be termed accidental or easily controllable variables, such as ratio of height to diameter of the test specimen, was specifically excluded. Possibly this assumption was too hastily made, and it might be both instructive and useful to endeavour to determine the various causes of Mohr envelope curvature, since the design procedure to be employed in each case might be somewhat different.

I am not convinced that we need to be unduly concerned with the shape of the part of a curved Mohr envelope to the left of its point of tangency with the Mohr circle representing the unconfined compressive strength to which Mr. Endersby has just referred. We

cannot explore the location of this portion of the Mohr envelope by means of the triaxial test in any case, although under certain conditions we might make use of the direct shear test for this purpose. It is the part of a curved Mohr envelope to the right of its point of tangency with the Mohr circle representing the unconfined compressive strength that is of primary concern, since this portion includes the stresses to which the pavement is actually subjected by traffic. As indicated in the paper itself, this part of the Mohr envelope can be represented by a parabolic equation. After the Mohr circle representing the conditions of stress for the most critical element within the pavement has been located, the tangent common to both it and the envelope provides the values of c and ϕ that are required for pavement design.

MR. C. A. CARPENTER: Mr. Chairman, I am glad Dr. McLeod left his circles on the board. In our experience, and I don't offer this as the final answer, but in our experience with this test, we have developed both straight Mohr envelopes and curved ones of the same type that Dr. McLeod is describing. Our experience is that we get our curvature when there is a change in the density of the specimens during the test. As the density of the specimen increases, and this occurs on workable type mixtures where compression, slowly applied, can cause some additional compaction, we get this gradual flattening of the friction curve. If compaction is related to the general tendency of that type of envelope to curve, then I don't believe the parabola has any particular bearing on the situation, because I think that at each point on the curve a tangent to the curve extending through an intercept on the Y ordinate represents the conditions in the mixture at that particular stage of compaction.

Now, if we are working with a mixture on which we know that the wheel loads will be light, say thirty pounds per square inch, we are interested in the slope and intercept for some comparable test condition, but if we are going to be dealing with two-hundred pound tire pressures then we should go out on the curve and determine the intercept and slope at a point corresponding to this loading.

PROF. VALLERGA (by letter): In the discussion following Dr. McLeod's excellent paper, it was brought out that his theoretical treatment of the subject of curved Mohr envelopes was based on test data which indicated both a definite curvature of the envelope and an intercept on the ordinate axis. My purpose in asking questions was to ascertain whether Dr. McLeod had considered the possibility that the test data he used were unduly influenced by

such things as the relative size of the aggregate particles compared to the size of the specimen, the manner of loading the specimen (including rate of loading), the effects of the confining rubber membrane (if one were used), the specimen dimensions, particle orientation, particle location, etc .

From data being accumulated at the University of California, it appears that this matter of triaxial testing of aggregates, with or without asphalt added, is still not a settled issue especially if one takes the view that the fundamental strength properties of the materials should be evaluated. The philosophies and techniques of triaxial testing are such that an intelligent interpretation of the results obtained requires a thorough knowledge of the specimens and all the details of test procedure. Furthermore, I am almost certain that the curvature of Mohr's envelope of failure and the apparent intercept on the ordinate for these materials are merely effects produced by particle size relative to specimen size, size of specimen, kind of loading, limitations of test equipment and instrumentation and, finally, improper interpretation of the test data. I submit that, when all of these factors are taken into account, the true envelope for any mass of granular material is a straight line which passes through the origin and whose inclination is a function of the resistance to sliding of particle on particle.

Interlocking is not a factor, I **believe**, because it is merely a manifestation of the frictional resistance between particles, In other words, with no friction there can be no interlocking in an aggregate mass. Also, I do not believe that the general **rule that** the specimen size should be at least four times the maximum dimension of the largest particle is sufficient to eliminate **all** the effects of large particles.

I am not prepared at this time to go into any further detailed discussion. The intent of these additional comments is to clarify and add to my remarks at the meeting.

DR. CHARLES MACK² (by letter) : Dr. McLeod is to be congratulated for his paper. This paper deserves special commendation for treating the case of a curved envelope to Mohr's stress circles in view of the general tendency to take only linear tangents into consideration. Defining by σ the stress normal to the shear plane, by σ_1 and σ_2 the principal compressive and tensile stresses, by τ the shearing stress along the plane, and by a the angle which the shear plane makes with the horizontal, then

$$\sigma = \frac{\sigma_1 + \sigma_2}{2} + \frac{\sigma_1 - \sigma_2}{2} \cos 2a \quad (1)$$

²Imperial Oil Ltd., Sarnia, Ontario.

$$\tau = \frac{\sigma_1 - \sigma_2}{2} \sin 2\alpha \quad (2)$$

giving the expressions for the normal and the shearing stresses in terms of the principal stresses. These equations hold, irrespective of whether α is constant or not. For the case of a constant, the tangent to the Mohr circles is linear and the shearing stress is

$$\tau = C + \sigma \tan \phi \quad (3)$$

Where C is usually termed "cohesion" and ϕ is the constant angle of internal friction ($\sigma = 45 + \phi/2$). The so-called cohesion is the intercept of the tangent on the τ axis and is a shearing stress, viz., the shearing stress τ_0 at $\sigma = 0$. This condition is fulfilled for a state of pure shear in the plane of **maximum** shearing stress, **where** $\sigma_1 = \sigma_0$, $\sigma_2 = -\sigma_0$ and $\alpha = 45^\circ$. Introducing these terms into eq. (1) and (2) gives $\sigma = 0$, $\tau_0 = \sigma_0$, and the "cohesion" is equal to the yield value. At stresses **smaller** than the yield value, the system is in the elastic region. In this region, the stresses **are** $\sigma_1 = \sigma_1$, $\sigma_2 = 0$, $\sigma = 0$, $\tau = 0$, and every particle retains its neighbors. At **stresses** in excess of the yield value, the system is in **the** plastic region. This type of deformation is accompanied by the formation of shear planes and shift of the particles,. In the simplest case, the shear plane makes an angle of 45° with the **horizontal** in the case of compression. If the shear is **accom-**panied by rotation, this angle becomes $45 + \phi/2$, 'where ϕ can be **constant** or variable. With $\phi = \text{constant}$ eq. (3) holds, with ϕ being variable, Dr. **McLeod's** treatment holds true, and the **envelope** to the stress circles is a curve. If the envelope is parabolic in shape, then in general

$$(\tau - \tau_0)^a = \beta \sigma \quad (4)$$

where a and B are constants. Dr. **McLeod** considered the special case of $a = 2$, however, a may have any value larger than **1**. The general eq. (4) becomes equal to eq. (3) with $a = 1$, $B = \tan \phi$. Another possible case is that the normal stress σ can. be an **ex-**ponential function of $\tau - \tau_0$. A variable angle ϕ is connected with structural changes in the material under stress.

In any part of the road structure, be it bituminous pavement, basecourse or subsoil, the particles are distributed at random, when the material is compacted under lateral constraint. The long axes of the particles make any angle with the horizontal. Loading of a material compacted in this manner will cause a rotation of the particles in the direction of plastic flow. This orientation is

accompanied by an increase in the value of the angle ϕ and by hardening as a function of stress and time as shown by the writer (C. Mack, Proe. A.A.P.T. Vol. 16, p. 264, 1947). The hardening effect can be also demonstrated by a curved envelope to the stress circles. Let A B in the attached diagram, Figure I be such an envelope. A tangent to a point C intersects the shearing stress axis at point D. Thus the shear resistance has increased from the original value $\tau_0 = OA$ to $\tau_1 = OD$.

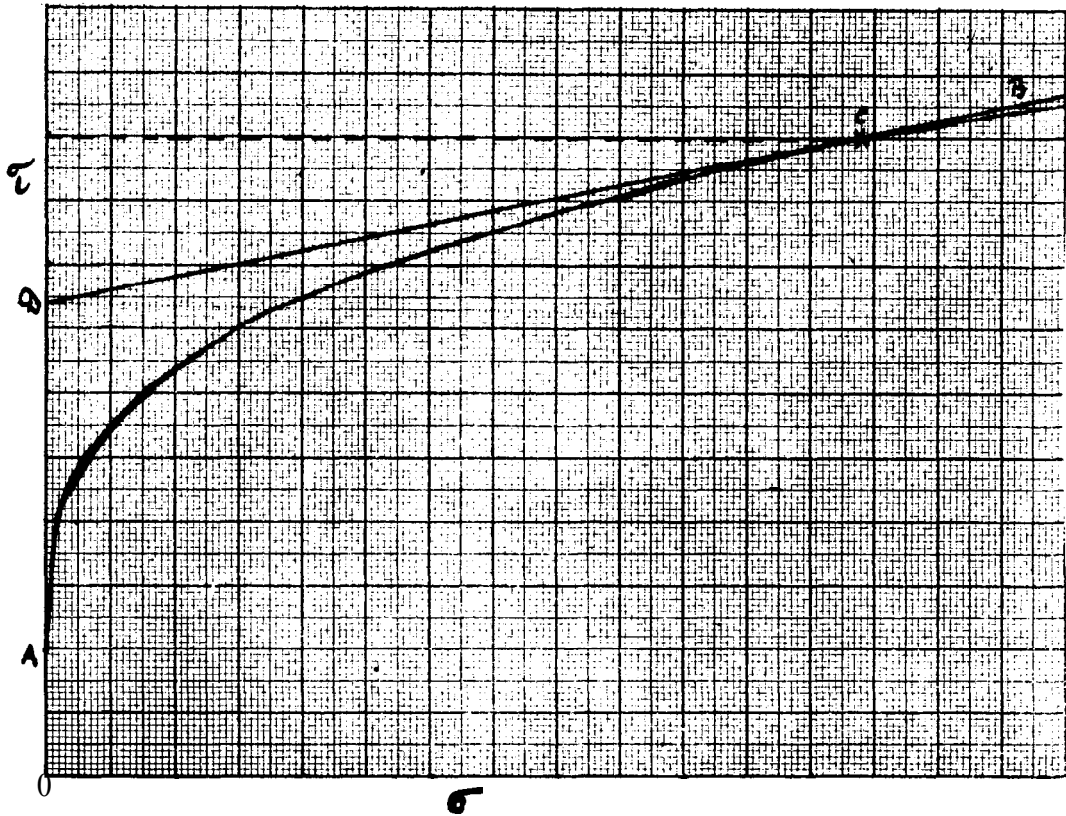


Fig. I

In the extreme case of orientation, all particles lie flat in the horizontal plane under compressive stresses. This process is accompanied by an increase of the angle $\alpha = 45^\circ + \phi/2$ from its original value to a final value of $\alpha = 45^\circ + \phi/2 = 45^\circ + 45^\circ = 90^\circ$, in which case, eq. (2) becomes

$$\tau = \frac{\sigma_1 - \sigma_2}{2} \sin 2\alpha = \frac{\sigma_1 - \sigma_2}{2} \sin 180^\circ = 0 \quad (5)$$

i.e., at this point, the shearing stress is zero, irrespective of the values of σ_1 and σ_2 . Hence the yield value of the material has increased from an original value of $\sigma_1 = \sigma_0$ to $\sigma_1 = \sigma$ max., and at this point, the material behaves like a solid under

compression within the elastic region. A rotation of the particles into a more orderly arrangement is accompanied by an increase in density. It is at this point where τ approaches zero or where the shear resistance has its maximum value, which determines the maximum strength of the material. At principal stresses, σ_1 and σ_2 , in excess of this point, the particles can rotate again and the density decreases. It can happen in this region that the envelope to the stress circles continues as a straight line. Such a behaviour has been demonstrated by Prof. Vallerga on the board for a subsoil. It has to be borne in mind, however, that it is the point of inflection which defines the maximum shear resistance, whereas an extrapolation of the linear Mohr envelope leads to a shear resistance of low or zero value.

Mohr's representation of stress is generally applied to data obtained from the so-called triaxial test, and a few remarks in this connection may be appropriate. The triaxial test is a compression test with simultaneous application of a lateral pressure. If compression develops a shear plane, then the compressive stress σ_1 , is accompanied by a tensile stress σ_2 acting at an angle of 90° to the direction of the compressive stress. Let the vertical pressure be $p_1 = \sigma_1$, and the lateral pressure p_2 . Taking the compressive stress with a positive and the tensile stress with a negative sign, it is generally assumed in the interpretation of the triaxial test (although not explicitly stated) that

$$\sigma_1 - \sigma_2 = p_1 + p_2 \quad (6)$$

or with $\sigma_1 = p_1$

$$- \sigma_2 = p_2 \quad (7)$$

This condition is met with the "closed" system, where the lateral pressure is allowed to build up as a result of the vertical pressure applied until equilibrium is reached. For the "open" system a lateral pressure of given magnitude is applied and kept constant. In this case, it remains doubtful whether eq. (7) is applicable or not, and to the writer's knowledge, no proof so far has been given in the literature for the validity of this assumption.

With regard to the operation of the open system cell, the test can be carried out to failure, at a constant rate of deformation or until a given rate of deformation is obtained. Since the test is carried out for the plastic region of the material, and plastic deformation is a function of time, it is only the latter two methods which take the time factor into consideration. It has been shown by the writer (see above reference) that for unconfined compression, the compressive stress is a function of the product of the

strain rate, $\dot{\epsilon} = d\epsilon/dt$ and of time t or, in general

$$\sigma_1 = f(\dot{\epsilon} t) \quad (8)$$

This equation holds also for the triaxial test, in which case σ_1 , has to be reduced by the lateral pressure. The time appears explicitly in eq. (8) because the mechanical behaviour of road structures, in which we are interested, depends upon their history. This history refers not only to the state of particle arrangement obtained by work done to the material previous to testing, but also to the manner in which the test is carried out. It can be shown from eq. (8) that the shear resistance increases with increasing strain-rate or rate of deformation, a result which gives the explanation as to why the compressive strength increases with increasing rate of deformation. The discussion in connection with the triaxial test may suffice to show that, as long as the **above-**mentioned factors are not taken into consideration, the test leads only to an accumulation of data which cannot be properly analyzed.

MR. H. G. NEVITT (by letter): Asphalt technologists should be greatly indebted to Mr. McLeod for his thorough and arduous efforts to fill in the gap between the sometimes highly theoretical concepts involved in laboratory or field testing and the actual action in practice of asphalt mats under traffic. The present paper spotlights some of the factors that exist in practice and may have important aspects in the application of test data to design in the field. It seems to the writer that **two** points in the discussion merit comment, as follows:

1 - The Lateral Restraining Effect of the Tire and the Base:

Mr. McLeod shows that any restraining effects by the tire and by the base underneath the mat which tend to restrict lateral flow of the mat can greatly increase the resistance to displacement exerted by that mat. 'His analysis shows that this is greatly dependent upon the amount of such restricting stresses, as influenced by the coefficient of friction, for example. His data indicates that, with such **coefficient** of friction falling anywhere within the range normally observed in actual tests, the resistance of the mat could be greatly increased. The corresponding implication is that, since such **coefficients** unquestionably exist, the tire and perhaps likewise the base do offer appreciable lateral resistance to displacement; and therefore such effects can be counted upon, at least as an added factor of safety.. This implied conclusion is in the writer's opinion entirely erroneous.

In his analysis Mr. McLeod ignores the fact that for a material to **create** a resisting stress a corresponding resisting

strain must first be built up. The amount of lateral movement required to create horizontal resisting stresses to the magnitude indicated by the analysis of the paper would involve lateral displacements so great that a considerable plastic flow would have occurred in the much less elastic pavement surface. It is true that, if plastic deformation to this degree did occur under the tire during its period of contact at that point, the lateral resistance visualized would be built up. However, I think it will be agreed that a surface which showed such displacement would be a highly unsatisfactory one even if, due to the tire resistance finally built up, further movement did not occur .

The lateral resistance which might be offered by the base is a rather different situation. Possibly the order of magnitude of the strains involved is sufficient to build up the stresses required without undue deformation in the mat. However, to limit the resisting strain to this magnitude may require in addition to the usual shearing and other resistances, some tensional resistance in the base as well; yet such tension is rarely observed except in the case of mats laid over rigid slabs. In fact, the surface mat is the one element in the usual flexible road structure which does have some ability to resist **tension**--dynamic at least--and therefore it seems difficult to consider the usual base under this mat as offering as much lateral resistance and hence resisting strains to such extent as to increase the resistance of the mat itself. If this theory (that the stability of the mat could be increased due to the presence of lateral stability in the layer below) is correct, it would be logical to consider the top inch of mat as able to resist the load for this reason and so on for each succeeding layer below. The possibilities are obviously so complex as to make the drawing of final conclusions difficult.

Mr. **McLeod's** analysis does have one very interesting and helpful conclusion, in that it shows a load applying medium which is capable of giving lateral resistance may **indicate** a much higher stability in the surface than would occur through the action of the ordinary pneumatic tire. A steel plate is exactly such a medium. Its coefficient of friction may not be high, but its very high coefficient of elasticity assures the building up of the lateral strain to the degree that this coefficient of friction permits. It therefore seems quite safe to conclude from Mr. **McLeod's** analysis that the resistance shown in plate bearing tests might be quite different from that offered to the actual tire, and for this reason (as well as others) the results from plate bearing tests need thorough and exact

correlation with the actual effects of load application through tires, such work reflecting field rather than laboratory conditions .

2 - General Theory: While the reasoning is less clear and exact, involving as it does the fundamentals of scientific philosophy, it seems to the writer that the very subject of Mr . **McLeod's** paper questions the validity of the method it outlines. An effort will be made to briefly present the reasoning behind this remark.

The basic premise of the triaxial determination of the angle of friction and cohesive strength of the aggregate-bitumen mix is that the relationship between the vertical and lateral stresses in the loaded pavement resisting displacement is the same as exists in the laboratory specimen when subjected to a uniform vertical loading and a simultaneous lateral pressure. The formulae relating these quantities given in the paper is true for an infinitesimal element at any point on a plane. For it to hold true throughout the sample mass, we must integrate these infinitesimal stresses over the area of this plane.

Obviously we cannot do this. The material is **non-homogeneous** and **non-isotropic**. It is impossible to evaluate the integral over the whole area in terms of constants for the composite material. Even if possible, such an integration would change for each plane passed through the point. We are therefore forced to the assumption that the material will act in practice in exactly the way an equivalent material which is homogeneous and isotropic and shows the same relation between the vertical and horizontal stresses at failure as the sample tested. Such an assumption might be quite valid, but its reliability must be appraised by further studies of the actual material in question. For example, a homogeneous and isotropic material which is not altered over the test range will give a Mohr envelope which is a straight line. The existence of such a straight line envelope has therefore been taken as one good bit of evidence that we could assume the quite unhomogeneous bituminous mix could be represented by analyzable material with which the theories of soil analysis could be applied and safely used. However, the fact that the Mohr envelope line is curved seems to the writer to be good evidence that the basic assumption involved in the analysis, and permitting the use of the equation of the article, is unsound; and therefore the applicability of these equations with any angle of friction and cohesion derived from the data is questionable .

It is, of course, quite possible that the action of the actual mix dealt with will be similar to that of some homogeneous and isotropic material with an unknown angle of friction and cohesive resistance; but to the writer it seems unsound to estimate its properties from the test characteristics displaced by the actual material at any point on the Mohr diagram. It must be remembered that the action of the sample under test is quite different from the action of the pavement under load. The sample has a uniform applied lateral pressure as well as a uniform vertical loading. In the actual pavement the stress may or may not be uniformly applied, but the resistance built up throughout the resisting mat varies throughout that mass. This resistance at any point is dependent upon the strain at that point, and this varies from a maximum at some point down to nothing; consequently the resistance of the mat is a composite effect involving resistance elements varying in stress intensity. The field stresses therefore concern every point on the Mohr envelope up to the point of maximum stress intensity; the cohesive resistance and angle of friction derived from some part of the Mohr diagram cannot be safely assumed that involved in the field resistance; the field resistance will be a composite effect, combining these varying constants in some unknown fashion.

The discussion of this point and the preceding one are characteristic of a situation which is often encountered in problems involving soils or similar materials. The assumptions made in the analysis, while appealing, represent what might occur rather than what assuredly does occur. Soils are two dimensional quantities, yet there is a continual effort to evaluate the resistance of soil by one constant. Bituminous mixtures have a highly involved internal structural action, yet there is a continual attempt to apply the relationships worked out for materials of extremely simple properties to them. It is perfectly sound engineering to attempt to correlate test properties of these mixes with their action in the field, but this **correlation** cannot depend upon assumptions which are appealing but not susceptible of proof. That such assumptions often seem to give excellent correlation for a certain proportion of the cases tested is not a justification for their use. We perhaps have a similar situation in another field of structural analysis. The theory of least work often results in stress calculations which are surprisingly close to those actually observed. It is a pleasing theory to assume a structure will so adjust its stresses that the minimum work is done in carrying the load, but elastic analysis shows that the structure does not always adopt this engaging

procedure. In the same way the application of the simple theory of soils has great appeal, and it is possible that it will be proven workably sound in the case of a straight Mohr envelope. It seems to the writer that its application in the case of curved envelopes must be preceded by convincing proof that this is justified, followed by confirming field correlations. Similar practical proof seems needed that tires supply appreciable lateral support to the pavement before this reinforcing effect can be counted on.

MR. McLEOD (author's closure by letter): The discussion of this paper by Messrs. Endersby, Vallerga, Carpenter, **Mack**, and Nevitt are greatly appreciated, for they have added much to the general subject under consideration, and have given emphasis to a number of points that clearly require further investigation.

It should be pointed out that several of those who have contributed to this discussion have referred to a problem that was considered to be outside the scope of the paper itself; namely, what factors are responsible for the curvature of the Mohr envelope. It is of interest to list the various causes of Mohr envelope curvature that have been suggested.

Professor Vallerga states that "the curvature of **Mohr's** envelope of failure and the apparent intercept on the ordinate for these materials are merely effects produced by particle size relative to specimen size, size of specimen, kind of loading, limitations of test equipment and instrumentation, and finally, improper interpretation of test data." Mr. Endersby believes that "this curvature represents that structural effect pure and simple, and the extent of it depends upon the dimensions of your sample." According to Mr. Carpenter, "we get our curvature when there is a change in the density of the specimens during test," while Dr. **Mack** states, "The hardening effect can also be demonstrated by a curved envelope to the stress circles."

It is quite apparent, therefore, that considerable difference of opinion exists concerning the cause of the curvature of the Mohr envelope. While the author recognizes the importance of this problem, little or no reference has been made to it in this paper because it could quite obviously be the subject of several articles by itself. For the present paper, it has been assumed that a curved Mohr envelope is a fundamental and not an accidental, fortuitous, or controllable characteristic of certain bituminous paving mixtures. The paper accepts this as a fact, without inquiring into the cause of the curvature, and proceeds to outline a method of design for such paving mixtures. The paper should be read with this distinction clearly in mind.

There are several theories of failure for various types of engineering materials, e.g., maximum shear stress, maximum normal stress, maximum normal strain, the internal friction theories of Coulomb and Mohr, etc. One or more of these theories may hold quite well for one class of engineering materials, but not for another. The Coulomb and Mohr internal friction theories seem to provide reasonable criteria of failure for soils, aggregates, bituminous paving mixtures, etc. They assume that shearing strength is due partly to a shearing resistance that can be developed even under zero normal stress and partly to a shearing resistance that consists of an internal resistance to sliding which is similar to friction in action. While the Coulomb theory of failure calls for a straight line relationship between shear and normal stresses, it should be carefully observed that **Mohr's** theory of failure does not specify either a straight line or curved envelope. Mohr left the shape of the envelope to be established by the experimental data for the material under test. Generally speaking, therefore, the Coulomb theory of failure, which specifies a straight line envelope, is simply a special case of the more comprehensive Mohr theory of failure.

The principal basis of support for the assumption of a straight line Mohr or Coulomb envelope when it occurs, is the fact that the triaxial or direct shear test data give a straight line envelope when plotted. Consequently, no further basis of support is required for the assumption of curved Mohr envelopes for certain bituminous mixtures than the fact that triaxial data for these paving mixtures provide Mohr diagrams for which the Mohr envelope is curved. In the latter case, the further assumption is made, at least as far as this paper is concerned, that the curvature of the Mohr envelope is a fundamental characteristic of certain paving mixtures, and is not due to controllable factors such as lack of adequate compaction, low ratio of height to diameter of the test specimens, etc.

Mr. Carpenter's brief account of his actual experience with the triaxial testing of bituminous paving mixtures provides a valuable addition to this discussion. He states that he has obtained both straight and curved Mohr envelopes and believes that curved envelopes are due to the increase in density of the test specimens as the triaxial test proceeds. As previously explained, in the paper itself curvature of the Mohr envelope due to inadequate compaction of the test specimen was ruled out as being an accidental or controllable, rather than a fundamental cause of **Mohr** envelope curvature. Mr. Carpenter's experience may indicate that this is a too rigid restriction.

Possibly the rather brief outline of the design of bituminous paving mixtures with curved Mohr envelopes given during the

presentation of the paper was not as clear as it should have been. However, the approach described was somewhat similar to that suggested by Mr. Carpenter. The Mohr circle representing the stress conditions for the element of pavement that will be subjected to the most critical loading anticipated in service must first be located on the Mohr diagram. The tangent to the curved envelope at its point of tangency with this critical Mohr circle gives the values for c and ϕ to be employed for design. As indicated in the paper, either a graphical or rigid mathematical method can be employed for this purpose. For the latter, it is necessary to assume that the portion of the curved Mohr envelope corresponding to the range of stress conditions under consideration can be represented by a parabolic or exponential, etc., type of mathematical equation, in order that the values for c and ϕ given by the tangent to the critical Mohr circle can be calculated.

In his written discussion, Professor Vallergera gives added emphasis to his point of view that for properly prepared and tested specimens of bituminous paving mixtures, the Mohr envelope is a straight line that passes through the origin. He suggests that either a straight or curved Mohr envelope that makes an intercept on the ordinate axis is an indication of improper specimen preparation or testing.

There is considerable evidence that this may be the case for cohesionless sand, gravel, etc. (See "Triaxial Shear Research and Pressure Distribution Studies," Waterways Experiment Station, Vicksburg, Mississippi.) On the other hand, when Professor Vallergera assumes that cohesion c (the intercept of the Mohr envelope on the ordinate axis) should always be zero, even after these aggregates have been mixed with bituminous binders to provide well-designed bituminous paving mixtures, he has reached a conclusion that is contrary to the findings of a considerable number of carefully conducted investigations.

In Volume 20 of the A.A.P.T. Proceedings, values for cohesion c up to about 40 psi. are shown in Figure 13 of the paper by Hennes and Wang. In the paper by Goetz and Chen in Volume 19 of the Proceedings, Figure 10 gives values for cohesion c as high as approximately 60 psi. In Figures 9, 10, and 11 in the paper by V. R. Smith in Volume 18, experimental data for various paving mixtures are plotted for which values for cohesion c up to about 22 psi. can be observed. Smith's data are of particular importance because the values for cohesion c were determined at essentially zero rate of strain during the triaxial test. This procedure provides minimum values for c since the viscous resistance factor is eliminated. Viscous resistance appears as an enlarged value for

cohesion c in the Mohr diagram for triaxial tests for which a positive rate of strain or deformation is employed. The paper by Nijboer in Volume 16 of the A.A.P.T. Proceedings contains data and graphs for triaxial tests on both sheet asphalt and asphaltic concrete types of bituminous paving mixtures. Nijboer's paper presents the results of an apparently very painstaking investigation, in which considerable trouble was taken to investigate almost every variable that might influence triaxial test results. In Graphs 1 and 2 of Nijboer's paper, Mohr envelopes for triaxial tests on sheet asphalt mixtures conducted at zero rate of strain give values for cohesion c of 15.6 and 31.2 psi. In Graph 4, for the same conditions of test, values for cohesion c up to about 40 psi. are shown for sheet asphaltic mixtures, and up to about 60 psi. for asphaltic concrete mixtures.

Furthermore, in Table 3 of his paper, Nijboer lists actual data showing that the addition of water to a dry sand provides the cohesive influence that we would expect from its **performance**. He demonstrates that this cohesive influence can be measured in a carefully run triaxial test. The value of cohesion c due to the moisture was 1.4 psi., when determined by triaxial tests on the moist sand that he investigated.

Nijboer endeavoured to eliminate any influence on his triaxial test results due to specimen dimensions, relation of largest particle size to specimen diameter, etc., which Professor Vallerga has suggested might be the cause of either an intercept on the ordinate axis (cohesion c), or curvature of the **Mohr** envelope. Consequently, Professor **Vallerga's** suggestion that the Mohr envelope for well-designed and properly tested bituminous paving mixture does not make an intercept on the ordinate axis appears to be contrary to existing published triaxial data., much of which has been very carefully obtained.

The various comments made by Dr. **Mack** merit serious consideration. As the triaxial test is ordinarily employed for the testing of bituminous paving mixtures, the terms "elastic region" and "yield value" do not have much significance, because it is their ultimate strength in the plastic rather than in the elastic region that is determined by the triaxial testing of these materials. The stress strain curves provided by the triaxial testing of bituminous paving mixtures are usually continuous curves, and it is difficult, if not impossible, to state with any exactitude what portion of the curve pertains to the elastic, and which to the plastic region. Consequently, Mohr diagrams for bituminous paving mixtures represent plastic and not elastic failure.

While Dr. **Mack's** equation (4) for a curved **Mohr** envelope could

be employed to obtain design data for bituminous paving mixtures, some preliminary-calculations tend to indicate that it would probably have no advantage over equation (25) selected in the paper to represent a curved Mohr envelope, and might be slightly more complicated to use .

Dr. Mack is entirely correct in pointing out that a time factor should be included in equations involving plastic deformation. However, his suggestion that triaxial data are of limited usefulness, unless this time factor is specifically included in their analysis, could arouse considerable debate insofar as practical solutions to engineering problems in flexible pavement design are concerned.

In the field of soil mechanics it has become customary to employ equations for plastic behaviour that do not contain the time variable. Errors due to this omission of the time factor may be more important in such precise fields as physics or pure rheology than to the solution of practical problems of engineering. It would be useful if someone would demonstrate by means of actual calculations for several practical examples whether or not the error involved by neglecting the time variable would exceed the factors of safety ordinarily employed by engineers. So far, in practical applications of soil mechanics, the error introduced by omitting the time variable from the equations employed has not been considered large enough to be serious. On the other hand, the time factor is ordinarily more or less inadvertently or indirectly taken into consideration when the triaxial test is run, since the test conditions employed in the laboratory are usually made to duplicate as nearly as possible the most critical conditions to which the material under test is likely to be subjected in the field. Consequently, the absence of a specific time variable in the equations for plastic behaviour usually employed for the analysis of triaxial data **is** probably very largely compensated for by endeavouring to have the triaxial test procedure duplicate field conditions.

The first points brought up in **Mr. Nevitt's** thoughtful discussion concern the frictional resistances between pavement and tire and between pavement and base as a source of additional bituminous pavement stability. Mr. Nevitt refers to these as the "lateral restraining effect of the tire and base," but in this closure they will be termed "frictional resistances," to conform to the terminology employed in the paper itself.

Mr. Nevitt suggests that the lateral strain within the pavement that would be required to provide sufficient frictional resistance between pavement and tire and between pavement and base to give any material increase in stability, would have to be so large that

the pavement itself would be damaged. In the absence of definite quantitative data, any opinions on this matter must be inferred from pavement performance and other sources.

In connection with his point of view, Mr. Nevitt states, "In his analysis, Mr. McLeod ignores the fact that for a material to create a resisting stress, a corresponding resisting strain must first be built up." The author suggests that Mr. Nevitt appears to have disregarded the fact that when a stress is applied to any material a corresponding strain is created within it. That the frictional resistance between pavement and tire, which is available for mobilization, may be of considerable magnitude, is indicated by the results of skid resistance tests made by Moyer and others, in which coefficients of friction between tire and pavement varying from 0.4 to 0.8 have been commonly measured. For a loaded truck tire inflated to 90 psi., this means that at the point of incipient skidding, the tire will exert an average horizontal stress of from 36 to 72 psi. on every square inch of its contact area on the pavement surface. Conversely, before a pavement could be squeezed out between this tire and a firm base, frictional resistances between pavement and tire of this order of magnitude must be overcome.

It is true that in these skid resistance tests the rubber tread of the pneumatic tire undergoes a much larger strain than the asphalt pavement, provided the shearing strength of the pavement is not exceeded. Nevertheless, in the ordinary operation of a tire on a pavement, some lateral strain occurs in the pavement due to the vertical pressure of the tire, and this lateral strain, even when relatively small, develops some frictional resistance between pavement and tire that tends to increase pavement stability. This is clearly indicated by published data for the Hveem Stabilometer and closed triaxial tests on bituminous paving mixtures. These tests demonstrate very convincingly that under even quite small vertical loads sufficient strain occurs in the test specimen to develop a measurable lateral pressure, and this lateral pressure is quite large for vertical loads approaching those exerted by truck tires. These lateral pressures are accompanied by corresponding lateral strains.

It is well-recognized that repeated small strains within bituminous pavements caused by traffic loads provide the kneading action that seems to be essential if these pavements are to remain in good condition. The strains necessary to permit this kneading action are, therefore, not detrimental to the pavement, and in addition they are a source of frictional resistance between pavement and tire that tends to contribute to pavement stability.

Mr. **Nevitt** also questions that frictional resistance between pavement and base is a source of pavement stability. The author is convinced that Mr. **Nevitt's** comments in this respect are thoroughly refuted by pavement performance in the field. It has long been known that if there is either no bond or a poor bond between pavement and base, pavement failure tends to occur due to sliding of the pavement on the base. Such failure also tends to take place whenever one layer of a bituminous pavement is poorly bonded to a lower layer. Consequently, within the author's experience, any suggestion that good frictional **resistance** between pavement and base is not an important source of pavement stability is entirely untenable.

The stability value given by a triaxial test on a paving mixture test specimen is its ultimate strength, which is developed only after some plastic flow has occurred. Mr. **Nevitt** is quite right in pointing out (and it was referred to in the paper itself) that the amount of plastic flow which takes place before this ultimate strength can be developed would result in so much lateral deformation of the pavement under the critical design load, that ultimate strength is not a satisfactory basis for actual design. Some safety factor must be applied to the ultimate strength as given by the triaxial test, in order that lateral deformation of the pavement under loaded tires can be kept within acceptable limits. However, the application of this safety factor only reduces the amount of strain that will develop under tires, and does not eliminate it. Even if such relatively large safety factors as 3 or 4 were applied to the coefficient of friction between pavement and tire as measured by Moyer and others, and if a coefficient of friction between pavement and base of the same order is assumed, the stability curves of Figures 11 and 14 demonstrate that for a wide contact area and relatively thin pavement, the frictional resistances between pavement and tire and between pavement and base would still be an important source of pavement stability.

It is a matter of common observation that the unsupported edge of a bituminous pavement will very often sustain traffic loads for years without collapsing, even when tires travel either along or partly over the edge. The author doubts that the extraordinary stability demonstrated in these cases is due merely to the inherent strength of the paving mixture itself, and believes they provide a practical demonstration of **the** important contribution of the frictional resistances between pavement and tire and between pavement and base pavement stability. From these various considerations, others referred to in the paper itself, and other observations of pavement performance in the field, the author has

concluded that the frictional resistances between pavement and tire and between pavement and base constitutes a potential source of substantial pavement stability.

Mr. Nevitt states that if these frictional resistances are an effective source of pavement stability, "it should be logical to consider the top inch of mat as able to resist load for this reason, and so on for each succeeding layer below." Possibly the **author** does not understand Mr. Nevitt's comment correctly, for its substance appears to be the equivalent of suggesting that if a column of material of a certain cross-section, and one foot long, will not fail under a given very heavy load, a similar column thirty feet long will also not fail or buckle under the same load. While the two cases are not parallel, it seems obvious that one can not apply this line of reasoning to either column design or pavement design.

In another part of his discussion, Mr. Nevitt states, "a homogeneous and isotropic material which is not altered over the test range will give a Mohr envelope which is a straight line." The paper by **Hennes** and Wang in last year's Proceedings makes it clear that the Mohr circles from triaxial data for a non-isotropic material (different shear strengths on the major and minor principal planes) are so located that a straight line tangent can be drawn to them also, although the points of tangency do not establish the positions of the failure planes. Consequently, a straight line tangent to the Mohr circles representing triaxial data does not necessarily provide a criterion of isotropy.

In the second part of his discussion, Mr. Nevitt suggests that the action of a sample under test in the laboratory may be different from that of a pavement under load in the field, and points out that a bituminous pavement may lack both homogeneity and isotropy. For these reasons, he questions that any values of c and ϕ obtained from a curved Mohr envelope can be selected for bituminous pavement design. Several of the objections raised by **Mr. Nevitt** are theoretically valid, but their practical importance should be assessed.

After a careful study of the effect of non-isotropy in bituminous paving mixtures, Hennes and Wang in their paper for last year's Proceedings (Volume 20) conclude, "Conventional interpretation of triaxial data probably gives a pretty reliable estimate of pavement stability, because of the 90° deflection of the slip surface in the case of pavement failure." In recent work at Vicksburg, the Corps of Engineers have been investigating stress strain curves obtained from large scale load tests on soil in the field, versus the stress strain curves provided by triaxial tests

on specimens of the same soil in the laboratory. They have been reasonably successful in developing a technique for the triaxial test, that provides stress strain curves in the laboratory approximating those resulting from the field load tests; that is, contrary to what Mr. Nevitt has suggested, the action of the sample during a properly conducted triaxial test in the laboratory may not be materially different from that of a pavement under load in the field. Furthermore, in connection with pavement design, the author questions Mr. Nevitt's statement that "the field stresses concern every point on the (curved) Mohr envelope up to the point of maximum stress intensity.' The author believes that there is only one point on the curved Mohr envelope in which we are greatly interested insofar as pavement design is concerned. This is the point of tangency between the Mohr circle representing the conditions of stress on the most critical element of pavement under the loaded area, and the envelope. On the basis of resistance to failure by squeezing out of the pavement between tire and base, this critical element is located on the contact area at the point where the pavement stability curve is just tangent to the tire pressure distribution curve, e.g., Figures 2, 13, 14, 15, 16, 29, etc. The c and ϕ values given by the tangent to the Mohr envelope at this point are the values to be employed in equations (18), (19), (20), or (21), as a basis for the design of the paving mixture. The value of the stability V required by this critical element is also provided directly by equations (43) or (44).

The author cannot concur with the sentiment contained in the last paragraph of Mr. **Nevitt's** discussion. No assumptions are made in the paper beyond those that are either commonly employed every day for the solutions of problems in soil mechanics, or that appear to have been already demonstrated to apply as a result of the observed performance of asphalt pavements in the field. It may turn out as Mr. Nevitt suggests, that the rational design of bituminous paving mixtures is an extremely complex matter. That remains to be demonstrated. At the present time, through the continued use of strictly empirical tests such as Marshall, Hveem, and Hubbard-Field, the asphalt paving industry has not taken even the first uncertain steps toward the adoption of a rational method of design, and it is quite apparent that the weaning process will not be easy, nor will it occur overnight. It seems reasonable at this time, therefore, that any proposed rational approach to bituminous pavement design should be presented in the simplest possible terms employing the simplest concepts., even though these are only approximate. After all, the scientific world progressed a long way on the relatively simple system of mechanics devised by Sir Isaac

Newton, which still provides solutions that are satisfactory for the vast majority of engineering problems in the applied mechanics field. It is for only special cases that the greater accuracy provided by the newer Einstein concepts of mechanics become important. Consequently, the author believes that at this time a rational approach to bituminous pavement design should be presented in the simplest possible form, even though it may be only approximately correct. If it should be found that a more complex approach is necessary for greater accuracy, it can be developed and applied later as required.